Angewandte Chemie
Eine Zeitschrift der Gesellschaft Deutscher Chemiker

Supporting Information

Broad Protection against Invasive Fungal Disease from a Nanobody Targeting the Active Site of Fungal β-1,3-Glucanosyltransferases

S. Redrado-Hernández, J. Macías-León, J. Castro-López, A. Belén Sanz, E. Dolader, M. Arias, A. M. González-Ramírez, D. Sánchez-Navarro, Y. Petryk, V. Farkaš, C. Vincke, S. Muyldermans, I. García-Barbazán, C. del Agua, O. Zaragoza, J. Arroyo, J. Pardo, E. M. Gálvez*, R. Hurtado-Guerrero**

Supplementary Information for

Broad Protection against Invasive Fungal Disease from a Nanobody Targeting the Active Site of Fungal β-1,3-Glucanosyltransferases

Sergio Redrado-Hernández[1,2$], Javier Macías-León[3$], Jorge Castro-López[3], Ana Belén Sanz[4], Elena Dolader[5,6], Maykel Arias[2,5,6], Andrés Manuel González-Ramírez[3], David Sánchez-Navarro[3], Yuliya Petryk[4], Vladimír Farkaš[7], Cécile Vincke[8], Serge Muyldermans[8], Irene García-Barbazán[9], Celia del Agua[10], Oscar Zaragoza[2,9], Javier Arroyo[4], Julián Pardo[2,5,6*], Eva M. Gálvez,[1,2*] and Ramon Hurtado-Guerrero[3,11,12*]

[$]These authors contributed equally: Javier Macías-León and Sergio Redrado-Hernández

*These authors share corresponding authorship. E-mail: rhurtado@bifi.es, pardojim@unizar.es and eva@icb.csic.es

Lead contact: rhurtado@bifi.es

This PDF file includes:

Reagent or Resource	Source	Reference
Recombinant DNA		
pPICZαGel4	GenScript	N/A
pPICZαGas2	GenScript	N/A
pHEN6c-U6270_NbGel4_3_MP57_Q15C	GenScript	N/A
pPICZaA-Nb3antiGel4-Fc-HisTag	GenScript	N/A
pHEN6cNb2	This manuscript	N/A
pHEN6cNb3	This manuscript	N/A
pHEN6cNb4	This manuscript	N/A
pHEN6cNb5	This manuscript	N/A
pHEN6cNb6	This manuscript	N/A
pHEN6cNb17	This manuscript	N/A
pHEN6cNb22	This manuscript	N/A
pHEN6cNb32	This manuscript	N/A
pHEN6cNb3-Cys	This manuscript	N/A
Bacterial and Fungal Strains		
E. coli DH5α	ThermoFisher	18265017
E. coli WK6	Thismanuscript	N/A
Pichia pastoris X33	ThermoFisher	C18000
A. fumigatus B5233	Provided by Dr June Kwon-Chung.	N/A
C. deneoformans 1229817	Provided by Dr. Antonio Rezusta – Hospital Universitario Miguel Servet.	N/A
A. fumigatus 1631562	Provided by Dr. Antonio Rezusta – Hospital Universitario Miguel Servet.	N/A
A. fumigatus 1677095	Provided by Dr. Antonio Rezusta – Hospital Universitario Miguel Servet.	N/A
A. fumigatus 1627666	Provided by Dr. Antonio Rezusta – Hospital Universitario Miguel Servet.	N/A
A. fumigatus 838	Provided by Dr. Antonio Rezusta – Hospital Universitario Miguel Servet.	N/A
A. fumigatus 286	Provided by Dr. Antonio Rezusta – Hospital Universitario Miguel Servet.	N/A
A. fumigatus 678715 (VRZ resistant)	Provided by Dr. Antonio Rezusta – Hospital Universitario Miguel Servet.	N/A
C. deneoformans JEC21	Provided by Oscar Zaragoza	[1]
C. deneoformans B3501	Provided by Oscar Zaragoza	[2]
C. deneoformans 24067	Provided by Oscar Zaragoza	[3]

C. neoformans KN99	Provided by Oscar Zaragoza	[4]
C. neoformans H99	Provided by Oscar Zaragoza	[5]
C. neoformans H99 CNAG06501- (*CnGel*-)	This manuscript	N/A
C. deneoformans acapsular (cap59)		[6]
C. neoformans acapsular (cap60)	Kind gift by Dr. James Kronstad	Unpublished.
C. albicans CAF2-1	This manuscript	[7]
E. coli OP50	*Caenorhabditis* Genetics Centre	N/A
Chemicals, Peptides, and Recombinant Proteins		
Cyclophosphamide	Sigma-Aldrich	Cat. # PHR1404
Hydrocortisone	Sigma-Aldrich	H0888
Voriconazole	Sigma-Aldrich	PZ0005
XTT	Panreac-AppliChem	A2240
Zeocin	Invivogen	ant-zn
Ampicillin sodium	Biosynth Carbosynth	AA44831
EndoH	This manuscript	N/A
PageRulerPrestained Protein Ladder	ThermoFisher	26616
*Sac*I HiFi	New EnglandBiolabs	R3156L
Isopropyl β-D-thiogalactopyranoside	BiosynthCarbosynth	EI05931
Sulfo-Cyanine5 maleimide	Lumiprobe	23380
Nourseothricin	Werner BioAgents, Jena, Germany	AB-102
NbSseK1	This manuscript	N/A
Nb2	This manuscript	N/A
Nb3	This manuscript	N/A
Nb4	This manuscript	N/A
Nb5	This manuscript	N/A
Nb6	This manuscript	N/A
Nb17	This manuscript	N/A
Nb22	This manuscript	N/A
Nb32	This manuscript	N/A
Nb3 (Q13C-Cy5)	This manuscript	N/A
Nb3-Fc	This manuscript	N/A
Gel4	This manuscript	N/A
Gas2	This manuscript	N/A
Gas1	Laura Popolo	N/A
Phr1	Laura Popolo	N/A
Phr2	Laura Popolo	N/A
Laminarin	Sigma	L9634-100MG
L6-SR	This manuscript	N/A
Caspofungin	Merck Sharp and Dohme [MSD] Research Laboratories, USA	N/A
Culture Media		

BHI powder	Sigma-Aldrich / Merck Millipore	Cat. # 110493
NGM Lite powder	US Biological Sciences	Cat. # N1005
RPMI 1640 broth w/o HCO_3^-	Sigma-Aldrich	Cat. # R7388
Sabouraud + Chloramphenicol	Sigma-Aldrich	Cat. # 89579
Critical Commercial Assays		
NucleoBondXtra Midi EF	MACHEREY-NAGEL	740420.50
AccuPrep Plasmid Mini Extraction Kit	BIONEER	K-3030
AccuPrep Gel Purification Kit	BIONEER	K-3035
FITC Conjugation Kit (Fast) – Lightning-Link	Abcam	AB188285
Animal models		
BALB/cJRj mice	Janvier	N/A
C. elegans AU37 (glp-4/sek-1 double mutant)	Caenorhabditis Genetics Centre	N/A
Deposited Data		
dGel4-Nb3 complex	Worldwide protein data bank	PDB entry 8PE2
dGel4-Nb4 complex	Worldwide protein data bank	PDB entry 8PE1
Software and Algorithms		
Origin 7	www.OriginLab.com	v7.0383 (B383)
GraphPad Prism	www.graphpad.com	v.8.0.1
Compusyn	www.combosyn.com	v.1.0
XDS	http://xds.mpimf-heidelberg.mpg.de/	[8]
SWISS-MODEL	https://swissmodel.expasy.org/	[9]
CCP4 software packages	www.ccp4.ac.uk/download/	[10]
Phaser	www.ccp4.ac.uk/download/	[11]
Coot	www.ccp4.ac.uk/download/	[12]
REFMAC5	www.ccp4.ac.uk/download/	[13]
Other		
HisTrap HP	Cytiva	11773209
HiPrep 26/10 Desalting column	Cytiva	GE17-5087-01
HiLoad 26/600 Supderdex 75 pg	Cytiva	GE28-9893-34
MBPTrap HP	Cytiva	28-9187-79
Cytiva Disposable PD-10 Desalting Columns	Cytiva	17-0851-01
PD Minitrap™ G-25	Merck Millipore	GE28-9180-07
Cassette PELLICON XL BIOMAX	Merck Millipore	PXB010A50
Auto-iTC200	Cytiva	N/A
Amicon Ultra CentrifugalFilters 10,000 MWCO	Merck Millipore	UFC901024
RPMI-1640	Lonza	BE12-702F

METHODS

Immunization and llama Nbs phage display library construction

An alpaca (*Vicugna pacos*) was immunized with six subcutaneous injections at a weekly interval with recombinant *A. fumigatus* deglycosylated Gel4 (100 µg/injection mixed with an equal volume of Gerbu adjuvants). Anticoagulated blood was taken from the jugular vein three days after the last boost with dGel4. After isolation of the peripheral blood lymphocytes and total RNA extraction, cDNA was prepared using commercial reagents[14]. VHH sequences were amplified from the cDNA through a nested PCR procedure[15]. The VHH amplicons were cut with restriction enzyme *Sap*I and ligated into the pMECS-GG phagemid following the Golden Gate Cloning strategy described by Romão et al.[15] A Nb DNA library ($7x10^8$ individual clones in the pMECS-GG phagemid) was generated in TG1 *E. coli* cells (Lucigen).

The library of phage-displayed VHHs, obtained after infection with M13K07 helper phages, was subsequently panned against solid-phase immobilized Gel4 recombinant protein[14]. Three rounds of panning were performed and enrichment of phages from wells with antigen relative to wells without antigen was noted after the second round. Crude extracts from 47 individual clones after the second and 47 individual clones after the third round of panning were screened against a Gel4-coated microtiter plate via ELISA. The Gel4 specific Nbs, ligated in frame and upstream of a hemagglutinin (HA)-tag and a His-tag were detected with a mouse anti-HA mAb (Biolegend) and an anti-mouse-AP conjugate (Bioké). More than 95% of each round scored positive for Gel4-specific binding.

After sequencing, the different Gel4-specific Nbs could be categorized into three different families based on the nature of their H3-sequence. Based on minor sequence variations among the Nbs within the same family, eight representative clones were chosen spread

over three families: Nb2, Nb4, Nb5, Nb6, Nb17, and Nb32 for family 1; Nb3 for family 2 and finally Nb22 for family 3 (Figure S1).

NbSsek1 was obtained using the same procedure described above but injecting on an alpaca the recombinant *Salmonella enterica* SseK1 (100 µg/injection mixed with an equal volume of Gerbu adjuvants).

Nanobody expression and purification

The nanobodies were expressed using the WK6 strain of *E. coli* in TB medium (2.3 g/L KH_2PO_4, 16.4 g/L K_2HPO_4, 12 g/L peptone, 24 g/L yeast extract, 0.4% glycerol, 5.5 mM glucose, 2 mM $MgCl_2$). First, a pre-culture (15 ml/L final volume) of TB supplemented with 100 µg/mL ampicillin was inoculated with the bacteria and incubated overnight at 37ºC and 220 rpm. The next day, the pre-culture was transferred to a 2 L culture of TB with 100 µg/mL ampicillin. Cells were grown at 37ºC and 180 rpm until the optical density at 600 nm reached between 0.6-0.8. Then, the culture was induced with 1 mM of Isopropyl-β-D-1-thiogalactopyranoside (IPTG) and the temperature was lowered to 28 ºC for overnight protein expression at 180 rpm. The culture was then centrifuged at 10,000 rpm for 20 minutes at 4ºC, and the cell pellet was frozen at -20ºC.

Nanobodies were extracted from the periplasm of the cell using 12 mL of TES buffer (0.2 M Tris pH 8.0, 0.5 mM EDTA, 0.5 M sucrose) per liter of culture. The cell suspension was incubated for 6 hours at 4ºC with constant stirring. Afterward, 24 mL of diluted TES (1/4 TES in water) were added, and the cell suspension was incubated overnight under the same conditions described above.

Cell suspensions were loaded into a HisTrap HP (GE Healthcare) column equilibrated in buffer 25 mM Tris pH 7.5, 300 mM NaCl, 10 mM imidazole. Nanobodies were eluted using an imidazole gradient from 10 mM to 500 mM. Imidazole was removed through

buffer exchange with a desalting HiPrep 26/10 Desalting column (GE Healthcare) to 25 mM Tris pH 7.5, 300 mM NaCl. The Nb fractions were pooled and concentrated to 2.5 mL using centrifugal filter units of 10,000 MWCO (Millipore). Finally, the isolated nanobody was further purified using a Superdex 75 XK26/60 column (GE Healthcare, Piscataway, NJ, USA) equilibrated with 25 mM Tris pH 7.5, 150 mM NaCl.

Labeling of Nb3 with Sulfo-Cyanine5 (Cy5) maleimide

The Nb3 Gln13 mutation to Cys was made by GenScript, and the mutant was expressed and purified as previously described, but with the addition of 2 mM DTT to the purification buffers to avoid potential oligomerization. The protein was then buffer exchanged to 25 mM Tris pH 7, 150 mM NaCl with TCEP (ten times the molar concentration of protein), and incubated for 30 minutes at room temperature. Subsequently, the Sulfo-Cyanine5 (Cy5) maleimide was added at a 1:10 ratio (protein:Cy5) and the mixture was incubated overnight at 4 ºC with gentle stirring. The next day, DTT was added to the mixture at a 1:10 ratio (Cy5 maleimide:DTT) to terminate the labeling reaction. The excess Cy5 maleimide was removed via a PD-10 Desalting Column, and the buffer was exchanged to 25 mM Tris pH 7.5, 150 mM NaCl. The concentration and percentage of labeled protein were determined by measuring its UV-visible region of the spectrum.

***A. fumigatus* Gel4 cloning, expression, and purification**

The DNA sequence encoding amino acid residues 19-504 of the *Aspergillus fumigatus* Gel4 was synthetically made and codon-optimized by GenScript for its expression in *Pichia pastoris.* The Gel4 sequence contains a His-tag at the 3′ C-terminus to facilitate purification. The plasmid (pPICZαA*Gel4*) was isolated from the *E. coli* strain DH5α,

linearized with *Sac*I, and used to transform the *Pichia pastoris* strain X33 (Invitrogen). Transformants were selected on YPDS plates (1% (w/v) yeast extract, 2% (w/v) peptone, 2% (w/v) dextrose, 1 M sorbitol) supplemented with 100 µg/mL zeocin (InvivoGen).

Cells expressing the glycosylated Gel4 (gGel4) were grown 24 h at 30ºC in BMGY medium (1% (w/v) yeast extract, 2% (w/v) peptone, 100 mM potassium phosphate pH 6.0, 1.34% (w/v) yeast nitrogen base without aminoacids, 1% (v/v) glycerol and 0.04% (w/v) biotin), then centrifuged at 4000 g for 10 minutes. The cells were resuspended in BMMY medium (1% (w/v) yeast extract, 2% (w/v) peptone 100 mM potassium phosphate pH 6.0, 1.34% (w/v) yeast nitrogen base without aminoacids, 1% (v/v) methanol and 0.04% (w/v) biotin) and incubated at room temperature. Supernatant containing gGel4 was collected after 72 h of methanol induction (adding 1% (v/v) methanol every 24 h) and concentrated to 20–50 mL using a Pellicon XL device (10,000 MWCO, PES membrane; Millipore), then dialyzed against 25 mM Tris pH 7.5, 300 mM NaCl, 10 mM imidazole.

The gGel4 sample was loaded onto a HisTrap HP (GE Healthcare) that had previously been equilibrated with 10 column volumes of 25 mM Tris pH 7.5, 300 mM NaCl, 10 mM imidazole. The protein was eluted in the presence of an imidazole gradient (from 10 to 500 mM) using the above buffer. Imidazole was removed with a HiPrep 26/10 Desalting column (GE Healthcare), using a buffer containing 25 mM Tris pH 7.5, 300 mM NaCl. Then gGel4 was treated with EndoH overnight at 18ºC, rendering the deglycosylated Gel4 (dGel4). This was verified with an SDS-PAGE, as shown in Figure S2A. After that, dGel4 was further purified by using a MBPTrap HP (GE Healthcare), previously equilibrated with 10 column volumes of 25 mM Tris pH 8.0, 150 mM NaCl, 1 mM EDTA, and collected in the flow through. The protein fraction was then concentrated to 2.5 mL using centrifugal filter units of 10,000 MWCO (Millipore). Subsequently, gel filtration

chromatography was carried out using Superdex 75 XK26/60 column (Cytiva) in 25 mM Tris pH 7.5, 50 mM NaCl. dGel4 was dialyzed in 25 mM Tris pH 7.5 and protein concentration measured by absorbance at 280 nm using an extinction coefficient of 70,555 $M^{-1}cm^{-1}$. The gGel4 used in our studies was further purified by gel filtration chromatography under the same conditions described for the dGel4 purification.

Nb3-Fc cloning, expression and purification

A DNA construct was designed to incorporate *Nb3* at the 5' end, along with a DNA sequence encoding a Gly linker, the IgG1 Fc region, and a His-tag. To enhance expression in *Pichia pastoris*, GenScript performed codon optimization. Subsequently, the construct was cloned into the pPICZαA vector using the *Xho*I and *Sac*II restriction sites.

This fusion protein was expressed and harvested using the same protocol as Gel4. The Nb3-Fc sample was loaded onto a HisTrap HP (GE Healthcare) equilibrated in with 25 mM Tris pH 7.5, 300 mM NaCl, 10 mM imidazole. The protein was eluted in the presence of an imidazole gradient (from 10 to 500 mM) using the above buffer. Imidazole was removed by performing buffer exchange using a HiPrep 26/10 Desalting column (GE Healthcare), with a buffer composition of 25 mM Tris pH 7.5, 150 mM NaCl. Afterwards, the protein was concentrated using centrifugal filter units of 10,000 MWCO (Millipore) and protein concentration was measured by absorbance at 280 nm using an extinction coefficient of 65320 M^{-1} cm^{-1}.

Purification of dGel4-Nb3 and dGel4-Nb4 complexes for crystallization purposes

dGel4 and Nb3/4 were incubated together at 4ºC for 30 min in a proportion of 1 mol of dGel4 versus 3 mol Nb3/4. To purify the two complexes from the excess of Nb3/4, size-exclusion chromatography purification (Superdex 75 XK26/60 column, GE Healthcare)

was performed in 25 mM Tris pH 7.5, 150 mM NaCl. The formation and purity of the complexes were analyzed by SDS-PAGE coomassie staining. All the fractions containing the complexes were then pooled, buffer-exchanged in 25 mM Tris pH 7.5, and concentrated using centrifugal filter units of 10,000 MWCO (Millipore).

*Sc*Gas2, Phr1 and Phr2 purification

The enzymes were purified according to a previously described protocol[16].

C. neoformans and *C. deneoformans Cn*Gel cloning, expression and purification

To express *Cn*Gel proteins, a fragment of 1410 pb (encoding amino acids residues from 21 to 490 of *Cn*Gel^{H99} and 20 to 489 of *Cn*Ge^{JEC21}, lacking the secretion signal and a dubious GPI-modification site) was amplified from total *Cryptococcus* mRNA by PCR using the sequence-specific primers containing *Xho*I and *Sac*II restriction sites and a 6xhis tag at the 3´ end (sequences available upon request). The amplified DNA fragments were digested with *Xho*I and *Sac*II and then cloned into the *P. pastoris* expression vector pPICZαA previously cleaved with the same enzymes to obtain pPICZαA*CnGel_H99* and pPICZαA*CnGel_JEC21*. The correct sequence of these constructions was verified by DNA sequencing. *P. pastoris* strain X33 (Invitrogen) was transformed with the plasmids, previously digested with *Sac*I. Transformants were selected on YPDS plates (1% (w/v) yeast extract, 2% (w/v) peptone, 2% (w/v) dextrose, 1 M sorbitol) supplemented with 100 µg/mL zeocin (InvivoGen). Protein production was performed as described for Gel4 although at 30ºC. Supernatant was concentrated using a centricon plus-70 device (10,000 MWCO; Millipore), and protein purification was performed using ProBondTM nickel-chelating resin (Novex, Life Technologies). Before binding, the resin was equilibrated with 20 mM Na_2HPO_4 pH 8.0 and 500 mM NaCl, then the sample was added to the resin

and incubated at 4 ºC for 3 h. After discarding the supernatant, the resin was washed with 20 mM phosphate pH 6, containing 500 mM NaCl, and proteins were eluted with 50 mM histidine solution pH 7.5. Finally, the eluted fraction was dialyzed against 25 mM Tris pH 7.5, 150 mM NaCl. To determine the purity of the recombinant proteins and the efficiency of the production, recombinant proteins were monitored by SDS/PAGE, and concentration was measured by absorbance at 280 nm.

Isothermal titration microcalorimetry (ITC)

ITC was used to characterize the interaction of gGel4 and dGel4with our Nbs. All experiments were carried out in an Auto-iTC200 (Microcal, Cytiva) at 25ºC with either form of Gel4 at 35 µM (placed in the syringe) and concentrations of Nbs at 5 µM (placed in the sample cell), in 25 mM Tris pH 7.5, 150mM NaCl. Data integration, correction and analysis were carried out in Origin 7 (Microcal). The data were fitted to a one-site equilibrium-binding model.

MicroScale Thermophoresis (MST)

Binding assays of Nb3 to *Cn*Gel^{H99} and *Cn*Gel^{JEC21} were studied with MST using a Monolith NT.115 Pico instrument (NanoTemper Technologies). Prior to the binding experiments, *Cn*Gel^{H99} and *Cn*Gel^{JEC21} were labeled with Alexa Fluor™ 647 NHS Ester using N-Hydroxysuccinimide (NHS)–ester chemistry, which reacts efficiently with the primary amines of proteins to form highly stable dye–protein conjugates. For *Cn*Gel^{H99} and *Cn*Gel^{JEC21} labeling, *Cn*Gel^{H99} and *Cn*Gel^{JEC21} concentration was adjusted to 20 µM using the labeling buffer (25 mM HEPES pH 8, 150 mM NaCl). Lower concentrations may result in a loss of coupling efficiency. The solid fluorescent dye was dissolved in 100% DMSO at a concentration of about 600 µM and mixed thoroughly. Before mixing

the protein and the dye, the concentration of the dye was adjusted to 3-fold concentration of the protein using the labeling buffer. Then, the protein and the fluorescent dye solutions were mixed in 1:1 ratio and incubated for 30 min at room temperature in the dark. Unreacted 'free' dye was eliminated using PD Minitrap™ G-25 desalting columns. The experiments were conducted in binding buffer (25 mM TRIS pH 7.5, 150 mM NaCl) using 5 nM of *Cn*Gel^{H99} or *Cn*Gel^{JEC21} and variable concentrations of the Nb3 ranging from 13.4 nM to 441 μM. The measurements were performed in premium capillaries at 25ºC using 40% laser power and 20% LED power in order to obtain optimized results. Dissociation constants (K_Ds) were calculated using MO Affinity analysis. The experiments were done in duplicate (n = 2 independent experiments).

Biochemical characterization of the β-1,3-glucanosyltransglycosylase activity *in vitro*

A fluorescent assay was performed following the protocol described before[17]. Laminarin (β-1,3-glucan) was used as the glucanosyl donor substrate, and β-1,3-glucan oligosaccharides fluorescently labelled with SR (sulforhodamine) served as acceptor substrates for either form of Gel4 and Gel4 orthologs in the presence or absence of Nbs. In this assay, the reaction products generated in the presence of the enzyme are applied to a cellulose filter paper and dried. Washing the paper with 66% aqueous ethanol removes the low-Mr reaction products and the unused fluorescent substrate, whereas the high-Mr transfer products remain adsorbed on the paper. An increase in fluorescence indicates the binding of the labelled L6-SR to the polymer fraction adsorbed to the filter paper and resistant to washing with 66% ethanol. The activity was determined using 30 μM SR-labeled laminarihexaose (L6-SR) as acceptor and 2.5 mg/mL laminarin as a donor in 50 mM citrate-phosphate buffer pH 6.0, and in some cases at pH 5.5. For Phr1 and

*Cn*Gel inhibition assays, reactions were performed at pH 7.2, and only in the case of experiments using *Cn*Gel proteins, the final concentration of L6-SR was lowered to 0.9 µM. The Gel4 orthologs used in this study were *C. albicans* Phr1, Phr2, *S. cerevisiae* Gas1 and Gas2 and *C. neoformans* *Cn*Gel^{H99} and *C. deneoformans* *Cn*Gel^{JEC21}. The final concentrations of gGel4/dGel4, Phr1, Phr2, Gas1, Gas2, and *Cn*Gel were 0.58 µM, 0.55 µM, 1.1 µM, 0.53 µM, 1.1 µM, and 0.50 µM, respectively. To calculate the IC_{50}s of Nb3 and Nb4 against gGel4/dGel4, Nb3 and Nb4 concentrations were varied from 125 to 2850 nM while gGel4/dGel4 concentration was fixed at 420 nM. Enzymatic activity was measured by quantification of the fluorescence on a FluoStar Omega Reader (BMH Labtech). All the reactions were performed at 37ºC. The IC50 values were calculated with GraphPad Prism 5.0 program (GraphPad Software, Inc.).

Crystallization and data collection

Crystals of the dGel4-Nb3 and dGel4-Nb4 complexes were grown by sitting drop experiments at 18°C by mixing 0.5 µL of protein solution (15 mg/mL of either dGel4-Nb3 or dGel4-Nb4 complexes, respectively, in 25 mM Tris pH = 7.5.) with an equal volume of a reservoir solution (10% NPS, 0.1 M buffer system 3 pH 8.5 and 30% precipitant P500MME_P20K for dGel4-Nb3 complex; and 10% Halogens, 0.1 M buffer system 3 pH 8.5 and 50% precipitant P500MME_P20K for dGel4-Nb4 complex; Molecular Dimensions). The crystals were cryoprotected in their mother liquor and flash-frozen in a nitrogen gas stream cooled to 100 K.

Structure determination and refinement

Diffraction data were collected on synchrotron beamlines I24 and I04-1 of the Diamond Light Source (Harwell Science and Innovation Campus, Oxfordshire, UK) at a

wavelength of 0.97 Å and a temperature of 100 K. Data were processed and scaled using XDS[8] and CCP4 software packages[10, 18]. Relevant statistics are given in Table S2. The crystal structures were solved by molecular replacement with Phaser[11] using the PDB entry 2W62as a template for Gel4 and Nb3/Nb4 models generated by SWISS-MODEL[9]. Initial phases were further improved by cycles of manual model building in Coot[12] and refinement with REFMAC5[13]. Further rounds of Coot and refinement with REFMAC5 were performed to obtain the final structure. However, in the case of the dGel4-Nb3 complex, amplitude based twin refinement was also performed. The final model was validated with PROCHECK, model statistics are given in Table S2. The asymmetric unit of the $P3_121$ and $P2_12_12_1$ crystals contained one molecule and two molecules of dGel4-Nb3 and dGel4-Nb4, respectively. The Ramachandran plot for the dGel4-Nb3 complex shows that 89.3%, 10.5%, 0.2% and 0% of the amino acids are in most favored, allowed, generously allowed and disallowed regions, respectively. The Ramachandran plot for the dGel4-Nb4 complex shows that 90.8%, 9.2%, 0% and 0%, of the amino acids are in most favored, allowed, generously allowed and disallowed regions, respectively. Coordinates and structure factors have been deposited under accession codes 8PE2 (dGel4-Nb3 complex) and 8PE1 (dGel4-Nb4 complex).

Sensitivity of *Candida albicans* to Nb3

Assays were performed on *Candida albicans* (CAF2-1 background) according to the microdilution broth procedure EUCAST-AFST2012 (EDef 7.2). The experiment with Nb3 was determined in 96-well microplates (flat bottom) in RPMI-1640 (with 2% glucose and pH 7.0 with MOPS). The tested Nb3 concentrations ranged from 0.037 to 38 μM. Two-fold serial dilutions were made for Nb3 and each well was inoculated with

$1.2x10^4$ *C. albicans* cells. The optical densities at 595 nm were measured after 48 h of static incubation at 37ºC on a microplate reader (Model 680, Bio-Rad, USA).

Aspergillus fumigatus and *Cryptococcus neoformans* strains

Aspergillus fumigatus B5233 is a clinical strain of invasive aspergillosis (IA) isolated from a patient with leukaemia and was kindly provided by June Kwon Chung[19]. *Cryptococcus deneoformans* B3501, JEC-21, 24067, and *C. neoformans* KN99 and H99 were provided by Oscar Zaragoza. *Cryptococcus deneoformans* 1229817 and *A. fumigatus* 678715, 1627666, 1631562, 1677095, 838 and 286 are clinical isolates obtained in Hospital Universitario Miguel Servet, Zaragoza, Spain.

To obtain a *C. neoformans* mutant lacking *Cn*Gel4 (CNAG_06501) in H99 strain, we constructed a disruption cassette using phusion PCR in which the coding sequence of the gene was replaced by the noursethricin resistance marker NAT^R. For this purpose, the following primers were designed:

1 TCGGGATAGGGAGAGACGATAC);
2 GCTTATGTGAGTCCTCCCTCTAGGAACTCGTCGCCATCAC);
3 GTGATGGCGACGAGTTCCTAGAGGGAGGACTCACATAAGC)
4 (GAATTACAAGATGAAGGCGTTGATGGAAGAGATGTAGAAACGAG
5: CTCGTTTCTACATCTCTTCCATCAACGCCTTCATCTTGTAATTC
6: GCACTTTTCAGTCCGCTATTTC

Primers 2/3 and 4/5 are complementary between them, and the grey underlined region anneals in the plasmid used to amplify the NAT market. To obtain the disruption cassette, the 5´ and 3´flanking regions of the gene were obtained by PCR using primers 1/2 and 5/6 respectively (1 µM) and 1.5 ng of genomic DNA from H99 strain as template. These fragments were amplified with Phusion High Fidelity Polymerase using the following conditions: 98ºC (2 min), 35 cycles of amplification (98ºC, 30 s / 72ºC, 1 min) followed by a final step at 72ºC (7 min). To amplify the NAT marker, we used as template plasmid

pPZP-NATcc (1 ng) [20], and the resistance marker was amplified by PCR using primers 3 and 4 (1 μM) with Phusion High Fidelity Polymerase. The PCR conditions were similar to the described above, but an annealing step at 55ºC (15 s) was included, and elongation time was 2 minutes.

The three fragments were purified and mixed at equal molar concentrations (around 0.15 picomols from each) to be used in the phusion PCR using oligonucleotides 1 and 6. This PCR was done using Prime Start HS DNA Polymerase (Takara), using the following conditions: 95ºC (2 min), 35 amplification cycles (95ºC, 30 s, and 72ºC, 4 min), followed by a final step at 72ºC (7 min).

The DNA cassette obtained was purified from gel, and around 3 μg were used to transform H99 strain using biolistic particle delivery systems using a Bio-Rad PDS 1000/He machine[21]. Colonies were selected on Sabouraud agar plates containing nourseothricin (Werner BioAgents, Jena, Germany) at 50 mg/L. Correct insertion was tested by PCR using external primers to the disruption cassette with primers that anneal at the NAT marker. For this purpose, the following primers were designed

7_CNAG_06501_F: AGCCTCTTATCGTCCTTTCC
8_CNAG_06501_R: GCTCAACTCGACGCCGAGCAG
9_NAT_F: GGTCACCAACGTTAACGCAC
10_NAT_R: GTACGAGACGACCACGAAGC

Correct integration was confirmed by amplification with primers 7/10 and 8/9 using DNA from the NAT-resistant colonies.

To try to disrupt the homologous gene in JEC21, we followed a similar strategy. We first identified the homolog (CNN02260) in this strain by doing a blast in fungidb.org with the protein sequence of the CNAG_06501 protein from H99. To make the disruption cassette, the following primers were designed:

01_CNN02260_F: TGAACTGCCCTTTAGGAGCG

02_NAT_CNN02260_R:

GCTTATGTGAGTCCTCCCGGCTGTGTTTGTCTCTCGGA

03_CNN02260_NAT_F

TCCGAGAGACAAACACAGCCGGGAGGACTCACATAAGC

04_CNN02260_NAT_R:

CCGACGACAGTGATCGACTTGAAGAGATGTAGAAACGAG

05_NAT_CNN02260_F:

CTCGTTTCTACATCTCTTCAAGTCGATCACTGTCGTCGG

06_CNN02260_R: TGAACGAGAGCCCTACCTGAC

As explained above, primers 02/03 and 04/05 are complementary and the grey region anneals in the plasmid to amplify the NAT marker. The PCRs to obtain the three DNA fragments and the final DNA Phusion, and the biolistic transformation conditions were identical as described above for the disruption of CNAG_06501 in H99 strain.

Aspergillus fumigatus culturing and conidial suspension

Aspergillus fumigatus B5233 was cultivated on solid Sabouraud-chloramphenicol agar plates (Sigma-Aldrich, St. Louis, Missouri) for 48 hours to generate an ample supply of spores. To isolate only the conidia from the agar plates, a careful scraping of the surface was performed using a sterile hyssop soaked in Tween-20 (Sigma-Aldrich, St. Louis, Missouri). The collected *Aspergillus* conidia on the swab were then suspended in a 10 mL plastic or glass tube containing 5 mL of PBS to dissolve the spores. The mixture was vortexed for 15 seconds to break apart any clumps of spores. Examining the prepared inoculum under a microscope was essential to ensure the absence of hyphae. The conidial

suspension was adjusted to a concentration of 2-2.5x10^6 CFU/mL, approximately equivalent to 1 McFarland standard. The concentration of conidia was verified either by counting on agar plates or by using a hemocytometer.

Cryptococcus neoformans and *C. deneoformans* culturing and suspension

The strains and isolates of the *C. neoformans* species complex were cultivated on Sabouraud-chloramphenicol agar plates (Sigma-Aldrich, St. Louis, Missouri) at 30°C for 7 days. Inoculums of yeast were prepared in 10 mL plastic or glass tubes filled with 5 mL of PBS. The yeast cells were counted using a haemocytometer, and the concentration of the inoculum was adjusted to 1x10^7 CFU/mL.

XTT reduction assay (Drug sensibility assay)

The antifungal activities of voriconazole (VCZ), fluconazole (FCZ), amphotericin B (AMB), caspofungin (CSF), Nb3, Nb2, Nb4, NbSsek1, and their combinations with varying concentrations of Nb3 were evaluated against *A. fumigatus* B5233, *C. neoformans* H99, and *C. deneoformans* 1229817 using a colorimetric XTT [(2,3)-bis(2-methoxy 4-nitro 5-sulfenyl)-2H-tetrazolium] reduction assay (AppliChem, Darmstadt, Germany). These experiments were conducted in RPMI 1640 medium supplemented with 2% glucose and 25 mM HEPES (Sigma-Aldrich, St. Louis, Missouri). Microtiter plates were incubated for 48 hours, following which 50 µL of 1 mg/mL XTT solution, supplemented with 125 µM menadione, was added to each well. The microtiter plates were further incubated for 2 hours before plate reading. Data analysis was performed using GraphPad software.

Determination of synergistic effects

The synergy of Nb3 in combination with AMB, VCZ, FCZ, and Nb4 was determined using the Fractional Inhibitory Concentration Index (FICI) method as previously described[22]. However, in this study, FICIs were calculated using MIC50 instead of MIC90, as Nb3 cannot inhibit growth beyond 90% with the concentrations employed in this particular research.

Single sugar cell wall composition assay

To obtain stationary phase cells of *C. neoformans* and *C. deneoformans*, cultures from 7-day-old agar plates incubated at 30°C were harvested. The cells were then cultured for 24 hours in 5 mL of RPMI 1640 medium containing 2% glucose and 25 mM HEPES, either with or without Nb3, at 30°C. Subsequently, the cells were centrifuged at 1200 *g* for 10 minutes, and the culture medium was removed by washing the cells five times. Using a vortex, the washed cells were vigorously shaken with glass beads in Eppendorf tubes. The liquid fraction was separated from the glass beads and centrifuged at 8000 g for 10 minutes. This process was repeated three times to ensure thorough washing. The pellet containing broken cell wall fragments was hydrolysed in 5M sulfuric acid for 2 hours at 95°C. The hydrolysed extracts of the cell wall were then diluted and/or neutralized using a saturated barium hydroxide solution. HPLC analysis of the extracts was carried out using a Shodex SH1011 column (Showa Denko K. K., Tokyo, Japan).

Confocal microscopy

Cells of *C. neoformans* and *C. deneoformans*, which were grown on Sabouraud agar for 7 days at 30ºC, were harvested and resuspended in 500 µL of PBS. They were then incubated at room temperature for 15 minutes with Nb3-Cy5 (*Cn*Gel), 18B7Ab-FITC

(anti-GXM antibody), and calcofluor white (chitin and β-1,3-glucan) to visualize the localization of Nb3-Cy5 within *Cryptococcus* cells. Monoclonal antibody 18B7[23] binds to the capsular component glucuronoxylomannan, and it was conjugated to FITC using the FITC Conjugation Kit (Fast) – Lightning-Link (Abcam, Reference AB188285). After staining, the cells were centrifuged for 5 minutes at 3000 *g* and washed 5 times. A 10 µL drop of the cell suspension was placed on a slide and covered with a coverslip. The ability of Nb3 to penetrate the *Cryptococcus* capsule was examined using a Zeiss LSM 880 (Zeiss, Jena, Germany) confocal microscope.

To assess calcofluor white intake into the fungal cell wall, cells of *C. deneoformans* 1229817 and B3501 and *C. neoformans* H99, and spores of *A. fumigatus* B5233 were cultured in RPMI 1640 for 24 h. After that, cells were labeled with calcofluor white for 15 minutes and washed 5 times by centrifugation at 3000 *g*. The stained cells and hyphae were placed in 8-well chambered slides (Ibidi Gmbh, Gräfelfing, Germany) and centrifuged at 1200 *g* for 5 min to send them to the bottom. Cell wall fluorescence was measured in a Zeiss LSM 880 confocal microscope with Zen Blue (Zeiss, Jena, Germany) software. Fluorescence was measured and related to complete yeast cells, in case of *Cryptococcus*, or to μm^2 of hyphae, in case of *Aspergillus*.

C. elegans culturing and synchronization

The *C. elegans* strain used in this study was the *glp-4/sek-1* double mutant[24]. The *glp-4* mutation in *C. elegans* inhibits progeny production when cultured at 25°C[25], while the *sek-1* mutation disrupts the function of a MAP kinase involved in pathogen defence, rendering the worms more susceptible to certain pathogens[26]. The *glp-4/sek-1* double mutant strain can be obtained from the *Caenorhabditis* Genetics Centre.

C. elegans worms were propagated on NGM agar plates with 50 µg/mL kanamycin and 100 µg/mL streptomycin at 20°C (NGM Lite, US Biological Life Sciences, Swampscott in Massachusetts, USA) using *E. coliOP50* as a food source. To ensure synchronized populations of worms for further experimentation, a synchronization process was performed. This involved killing the larvae and adult worms and disrupting the *C. elegans* cuticle using a bleaching solution to release the eggs from gravid worms. The eggs are more resistant to harsh conditions compared to the worms themselves, and careful optimization of the bleaching and caustic substance concentrations is crucial for obtaining viable eggs. Once the eggs were obtained through synchronization, a pool of similarly aged and developed worms was collected. It is important to observe the presence of gravid worms under a dissecting microscope to determine the appropriate day for synchronization. Various factors, such as the ratio of worms to sodium hydroxide, the duration of contact between worms and bleaching solutions, temperature, and aeration of the eggs, can influence the success of obtaining viable eggs[27].

To synchronize *C. elegans* worms, the following steps were performed. Firstly, three 100 mm NGM agar plates were washed with 6 mL of M9 buffer containing Na_2HPO_4, NaCl, KH_2PO_4, and $MgSO_4$. The worm suspension in M9 buffer was then transferred to 15 mL Falcon tubes. If any eggs were stuck to the NGM agar plates, an additional 4 mL of M9 buffer was used to detach them. The tube containing the worm suspension was centrifuged at 650 *g* for 2 minutes, and the supernatant was discarded until only 2 mL of liquid remained in the tube.

Next, a bleaching solution consisting of 0.25 M NaOH and freshly prepared 1% NaClO was added to the worms, bringing the final volume up to 4 mL. The worm and bleaching solution mixture was vortexed for ten seconds, and a sample was taken to examine the worms under a dissecting microscope. If some worms were still alive or the majority of

their cuticles were intact, additional 10-second vortexing intervals could be required, up to a maximum contact time of 6 minutes. If the worm suspension contained a high number of worms, a higher concentration of NaOH might be necessary to break their cuticles. Regular monitoring of the worms under a dissecting microscope provided guidance on when to stop the bleaching process.

C. elegans L4 larvae culturing and infection

The L1 larvae obtained from synchronization were cultured at 25°C until they developed into L4 stage worms. Once the worms reached the L4 stage, they were transferred to a new NGM agar plate without any food source by washing the original plate. For the infection with *A. fumigatus* B5233, a 5 mL suspension of fungal conidia was prepared and then centrifuged for 2 minutes at 800 *g* to collect and sediment the spores. Subsequently, 50 µL of the conidial pellet was added to the NGM agar plate containing the L4 worms. The conidial droplet was placed on an area away from the center of the plate and allowed to dry. Two additional droplets were placed near the first one to ensure consistent infection. In the case of *C. deneoformans*, the infection was achieved by transferring the L4 worms onto NGM agar plates that already contained a lawn of yeast as a source of food for the worms. Both fungi and L4 worms containing NGM agar plates were cultured at 25°C overnight.

C. elegans survival assay

After the L4 worms were infected and incubated on the respective plates, they were harvested and washed six times with M9 buffer to remove any non-ingested fungal cells. Approximately 20 infected worms per well were then placed in a 96-well flat-bottom microtiter plate. Each well of the microtiter plate contained 20% BHI broth (Brain Heart

Infusion broth) and one of the following treatments: 4 µg/mL VCZ, 32 µg/mL FCZ, 0.25 µg/mL AMB, 32 µg/mL CSF, or 1 mg/mL Nb3. These concentrations were chosen for the assay. A total of 60 worms (distributed in 3 wells) were assessed for each concentration of the antifungal agents or Nb3. The infected worms without Nb3 treatment served as negative controls. The survival assays were carried out for 2 days at 25°C, and the survival of the worms was monitored every 12 h using a dissecting microscope (Leica EZ4). The number of surviving worms was recorded and analysed to evaluate the efficacy of each treatment in promoting worm survival.

In a separate experiment, the efficacy of different concentrations of Nb3 (ranging from 0.02 mg/mL to 8 mg/mL) in promoting the survival of L4 worms infected as described above was assessed. Similarly, a total of 60 worms were evaluated for each concentration, and the assays were repeated three times to ensure reliability and consistency of the results.

Aspergillosis and cryptococcosis murine model

Female BALB/c mice were given 200 mg/Kg of hydrocortisone through intraperitoneal (IP) injection to suppress their immune systems on days -2 and 0, and once a week after infection. On day 0, the mice were infected intranasally (IN) with 20 µL of PBS containing $2.5 \cdot 10^7$ CFU of *C. deneoformans* 1229817. The mice were then divided into three groups: one group received a vehicle (PBS) treatment (n=24), another group was treated with Nb3 at a dosage of 20 mg/Kg (n=24), and the third group was treated with NbSsek1 at a dosage of 20 mg/Kg (n=24). Half of the mice in each group received their treatment intraperitoneally (IP) while the other half received it IN. The treatments were administered three times a week for the duration of the experiment. On day 14 post-infection, six mice from each final group (a total of 36 mice) were sacrificed and their

fungal burden was assessed by counting agar plates containing serial dilutions from brain and lung homogenates. The plates were cultured for 24-48 hours at 30°C.

In another experiment, 18 mice were immunosuppressed with hydrocortisone, infected with *C. deneoformans*, and treated IN with either a vehicle, Nb3, or NbSsek1. After 14 days, their brains and lungs were removed and homogenized. The concentrations of Nb3 and NbSseK1 in the organ homogenates were determined using a His-Tag ELISA detection kit (GenScript, Piscataway, New Jersey) following the manufacturer's instructions.

For *A. fumigatus* B5233 infection, 36 female BALB/c mice were infected IN with 20 µL of PBS containing $1 \cdot 10^6$ CFU of *A. fumigatus* and divided into three groups (n = 12). Immunosuppression was achieved by administering cyclophosphamide at a dosage of 150 mg/Kg IP on days -3 and 0 and hydrocortisone on days 0, 2 and 4. Mice treated IN received a daily dose of 20 mg/Kg of Nb3 for one week while those treated IP received a daily dose of 80 mg/Kg. Six mice from the IN-treated group were sacrificed on day 4 post-infection, and their fungal burden was assessed using qPCR.

In a parallel experiment, 12 mice were infected with *A. fumigatus*, while another 12 mice were infected with *C. deneoformans*. These mice were then treated intraperitoneally with vehicle or Nb3 (80 mg/Kg for *A. fumigatus* and 20 mg/Kg for *C. deneoformans*). The mice infected with *A. fumigatus* and *C. deneoformans* were sacrificed three and fourteen days after infection, respectively, and their lungs were removed for hematoxylin eosin staining. Following fixation in 4% paraformaldehyde in PBS, the lungs were processed and stained with hematoxylin-eosin. Histological sections of the lungs were examined by an expert pathologist in a blind fashion to assess lung damage. The evaluation was based on a previously published scoring system[28], which assigned scores ranging from 0 to 4 based on the severity of the following parameters: endothelitis, edema, bronchitis,

necrosis, alveolar inflammation, interstitial inflammation, pleuritis, and hemorrhage. The extent of damage was assessed across the entire lung section and adjusted to represent the percentage of the lung surface affected. Each parameter was graded, and the total pathology scores were calculated as the sum of scores for all parameters.

In a previous set of experiments, similar patterns and dosages of Nb3 or vehicle were administered to immunosuppressed mice that were similarly infected with *C. deneoformans* or *A. fumigatus* but with the exception that these experiments were conducted under prophylactic conditions. The mice were immunosuppressed and infected as described before, and Nb3 or vehicle was administered IP or IN following similar dosages and schedules. The purpose of these experiments was to evaluate the prophylactic efficacy of Nb3 in preventing fungal infections.

In order to evaluate the effectiveness of Nb2 against fungal infections, 24 female BALB/c mice were split into two groups of 12 mice each. One group was given cyclophosphamide and hydrocortisone, while the other group only received hydrocortisone. Afterwards, the mice were infected with *A. fumigatus* or *C. deneoformans*, following the same procedure as previous experiments. Six mice infected with *A. fumigatus* were given IN vehicle daily and served as a control, while the other six were given IN Nb2 daily for a week. Similarly, half of the mice infected with *C. deneoformans* were treated with IN Nb2, while the remaining half received IN vehicle three days a week until the end of the experiment.

IISA and CSIC adhere to all protocols set by the Committee of Animal Experimentation of the University of Zaragoza, accredited as the Body in Charge of Animal Welfare (OEBA). All experimental procedures comply with FELASA guidelines. In handling animals, we follow the 4Rs rule (Reduction, Refinement, Replacement, and Responsibility) as mandated by Royal Decree 53/2013, dated February 1. The degree of animal suffering and/or pain is monitored using the Morton and Griffiths scales, and

appropriate measures, such as analgesia or euthanasia, are administered as necessary. Permissions for these procedures were granted under PI33/20 and PI44/20.

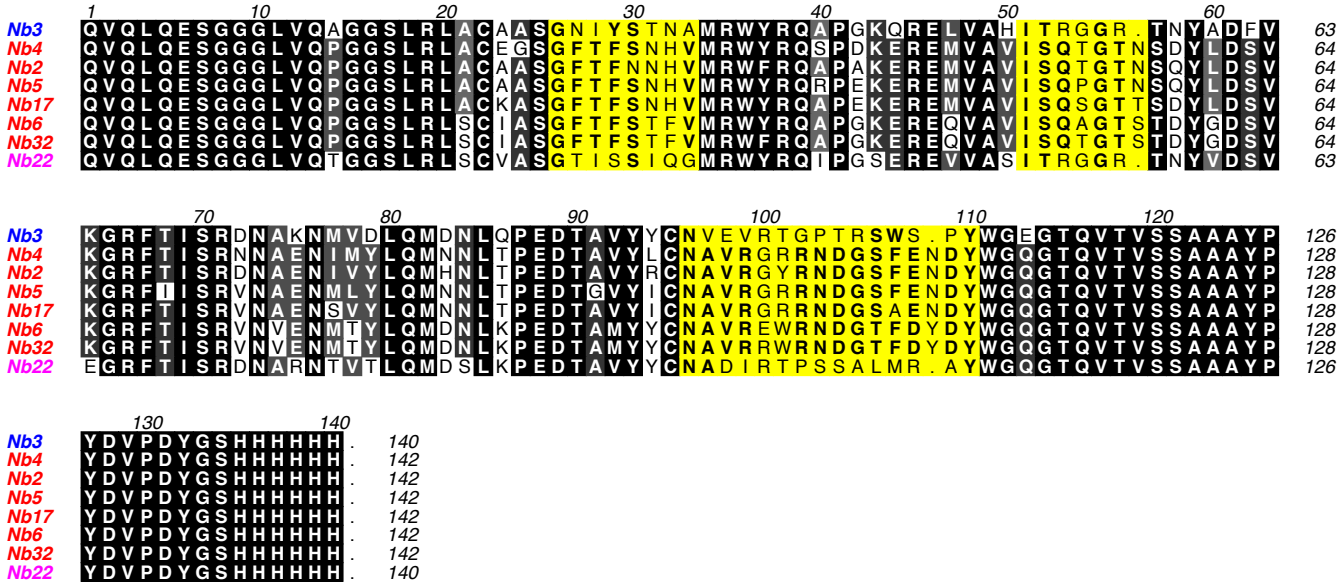

Figure S1. Multiple alignment of the selected anti-Gel4 Nbs. The names of the Nbs grouped in the three families are indicated by blue, red, and pink, respectively. Nb2/4/5/17/6/32, Nb3, and Nb22 belong to families 1, 2, and 3, respectively. The three hypervariable loops of the Nbs are highlighted in yellow. Nbs, due to their convex and compact shape together with their H3 of unusual length (around position 100), are capable of binding specifically to structured, often cryptic epitopes that are frequently inaccessible to conventional antibodies (e.g. enzyme active sites)[29].

A

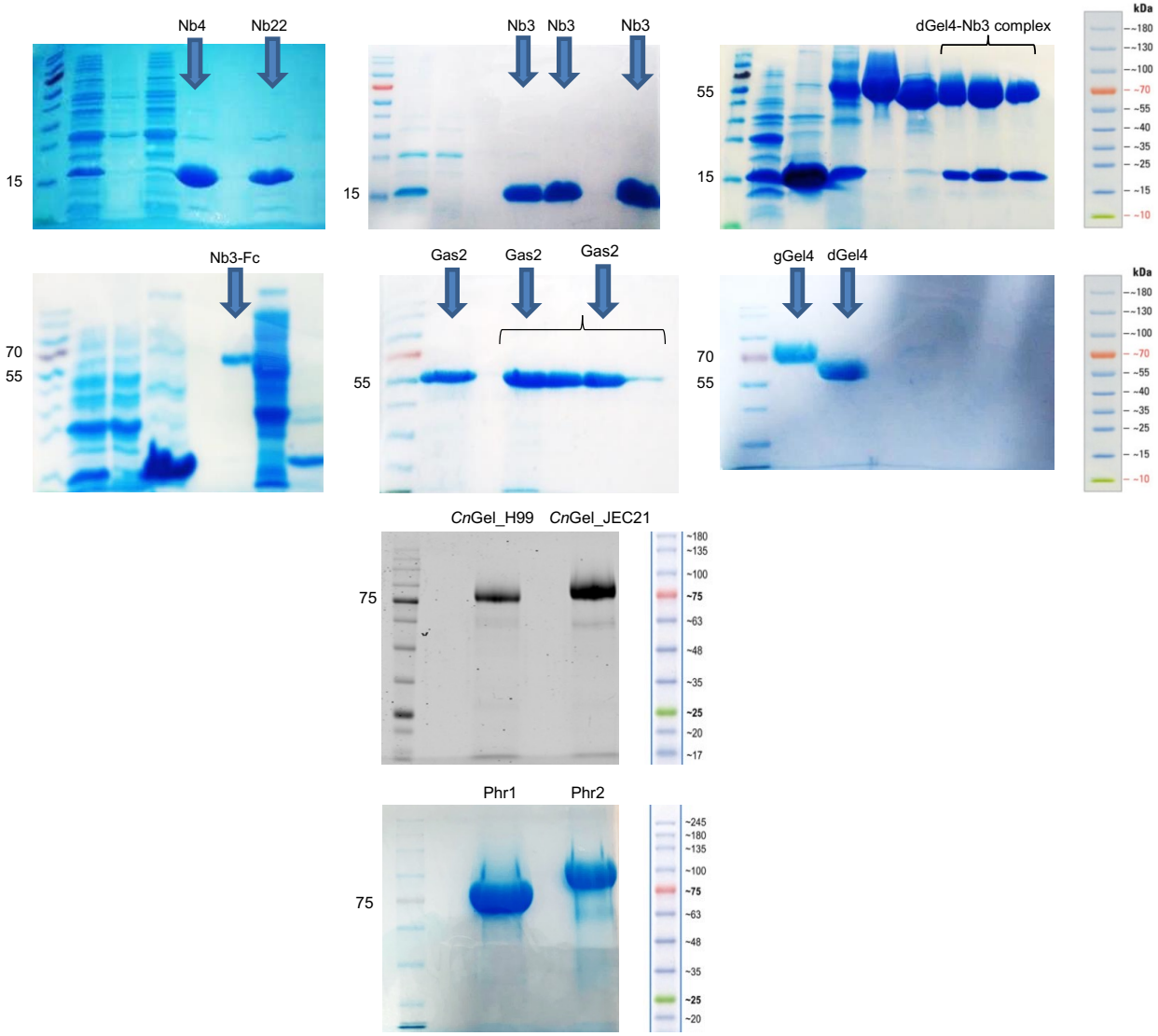
Nb4
Nb22
15
Nb3
Nb3
Nb3
15
dGel4-Nb3 complex
55
15
kDa
~180
~130
~100
~70
~55
~40
~35
~25
~15
~10
Nb3-Fc
70
55
Gas2
Gas2
Gas2
55
gGel4
dGel4
70
55
kDa
~180
~130
~100
~70
~55
~40
~35
~25
~15
~10
CnGel_H99
CnGel_JEC21
75
~180
~135
~100
~75
~63
~48
~35
~25
~20
~17
Phr1
Phr2
75
~245
~180
~135
~100
~75
~63
~48
~35
~25
~20

B

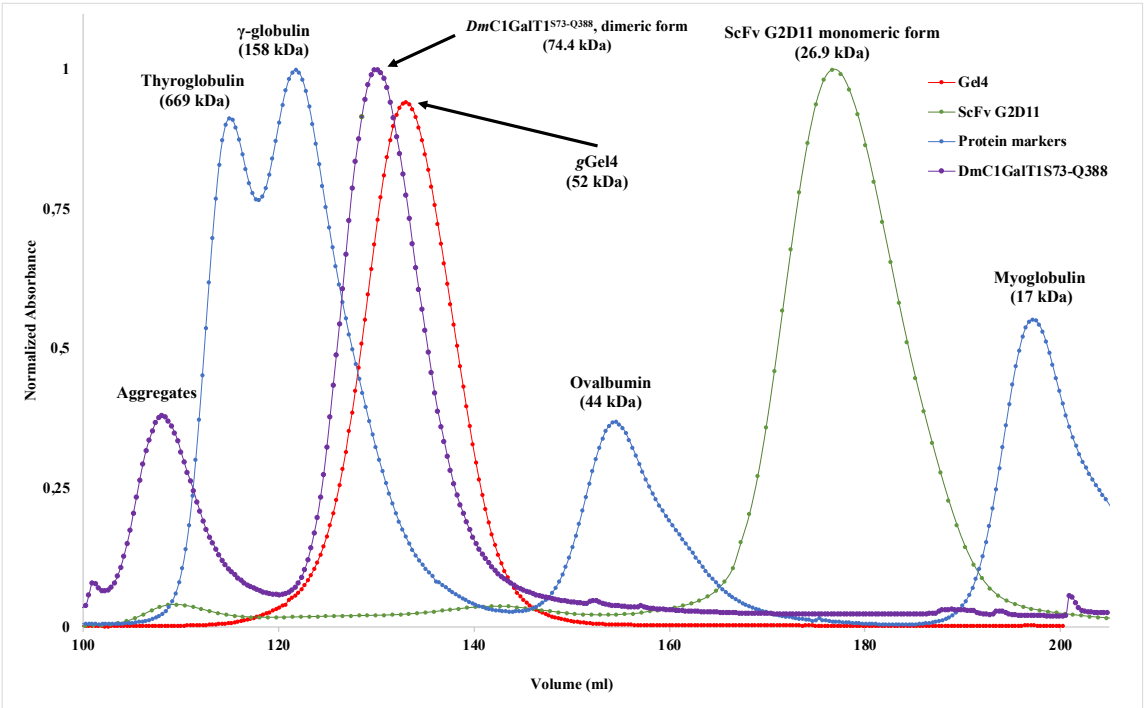
γ-globulin
(158 kDa)
DmC1GalT1S73-Q388, dimeric form
(74.4 kDa)
ScFv G2D11 monomeric form
(26.9 kDa)
Thyroglobulin
(669 kDa)
gGel4
(52 kDa)
Gel4
ScFv G2D11
Protein markers
DmC1GalT1S73-Q388
Myoglobulin
(17 kDa)
Aggregates
Ovalbumin
(44 kDa)
Normalized Absorbance
1
0,75
0,5
0,25
0
100
120
140
160
180
200
Volume (ml)

Figure S2. (A) SDS-PAGE gels showing the purity of some of our β-1,3-glucanosyltransferases and Nbs. Note that the purity of the dGel4-Nb3 complex is also depicted. The SDS-PAGE gels also demonstrate that the dGel4-Nb3 complex is pure and that the trimming of N-glycans present in gGel4 is verified by the shift in the molecular weight of gGel4 upon treatment with EndoH. The purity for Nb3-Fc is also shown. The SDS-PAGE gels feature a variety of proteins unrelated to the transglycosylases and Nbs under study. As a result, we have refrained from annotating the lanes corresponding to other proteins. (**B**) Analysis of gGel4 by size exclusion chromatography. The chromatogram shows several protein markers with their molecular weights and the monomeric form for gGel4. Note that we have also added the dimeric form of *Dm*C1GalT1[30] to demonstrate further that gGel4 is monomeric.

Family 1

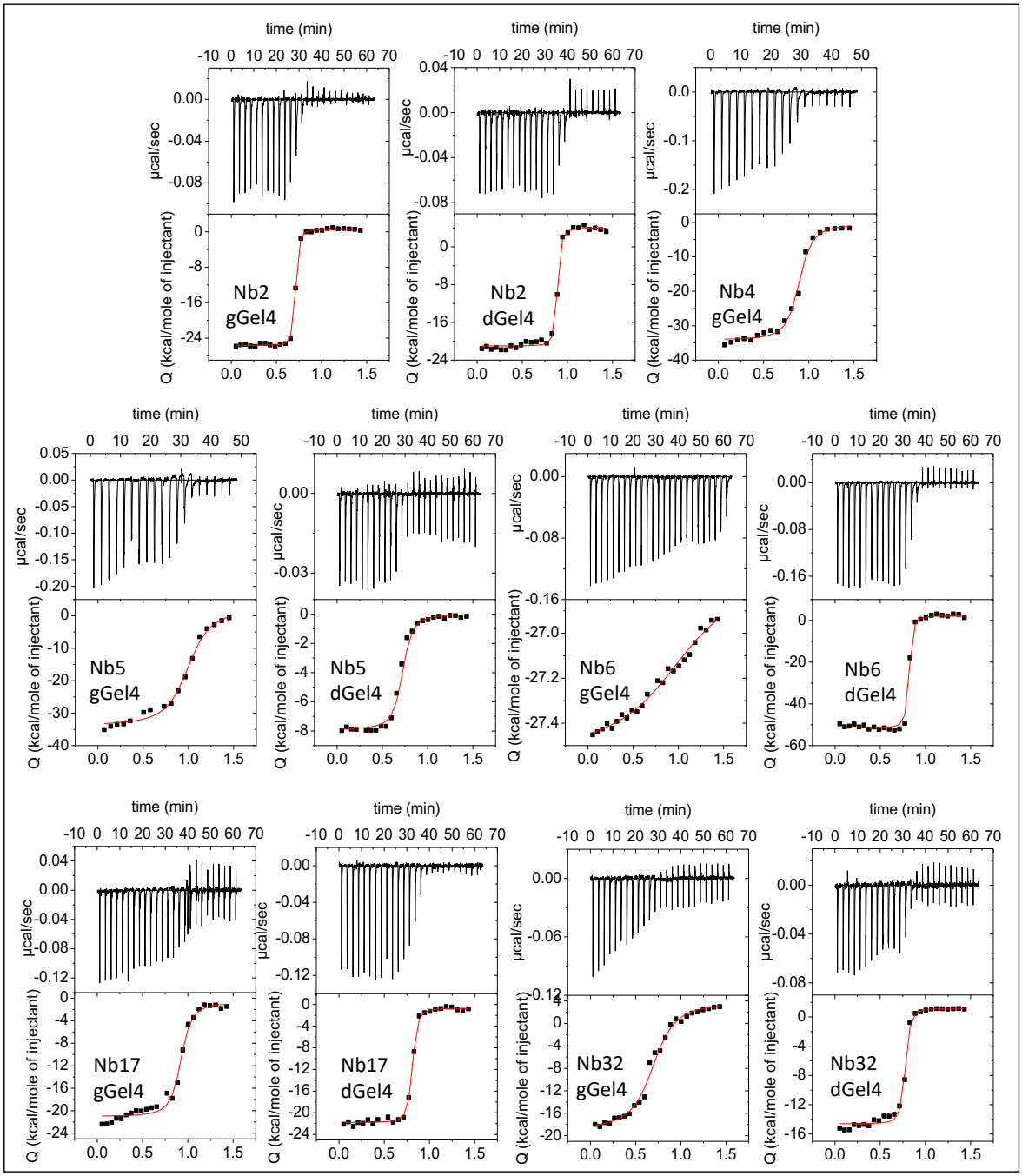

Family 2

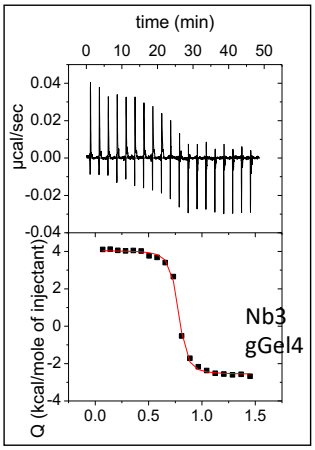

Family 3

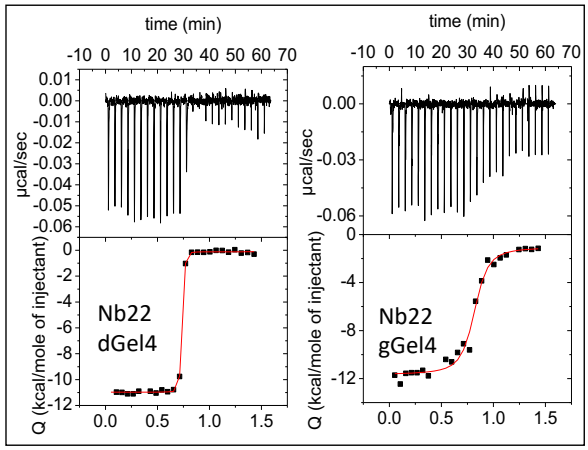

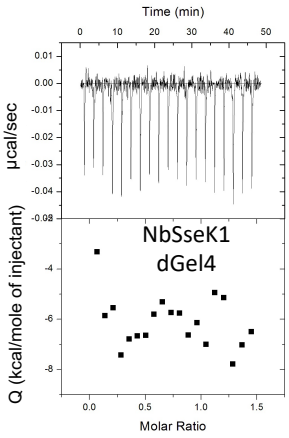

Figure S3. ITC data for the binding of Nbs to gGel4 and dGel4. Top: raw thermogram (thermal power versus time). Bottom: binding isotherm (normalized heats versus molar ratio). See Table S1 for the thermodynamic and K_D values for all Nbs. Note that gGel4 and dGel4 stand for glycosylated and deglycosylated Gel4, respectively. The experiments were performed in duplicate (n = 2 independent experiments).

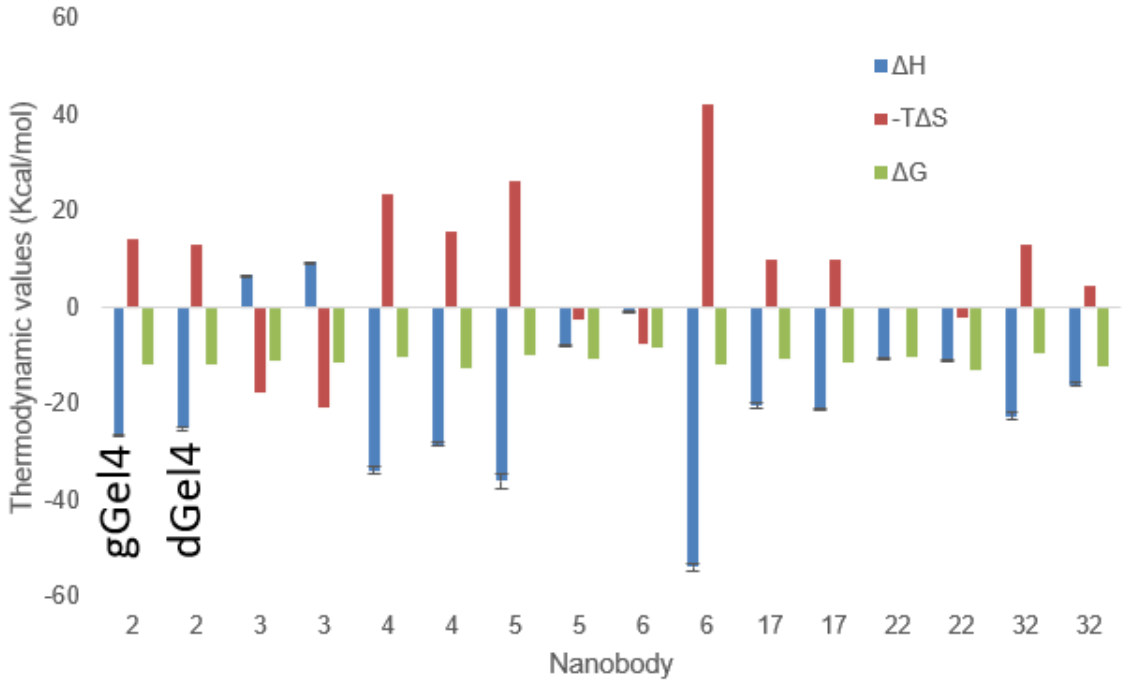

Figure S4. Thermodynamic dissection of the interaction of gGel4 and dGel4 with Nbs. The binding Gibbs energy (ΔG), enthalpy (ΔH), and entropy (–TΔS) are represented in green, blue, and red bars, respectively. The thermodynamic parameters are in kcal/mol. Any negative value represents a favorable contribution to the binding, whereas a positive value represents an unfavorable contribution.

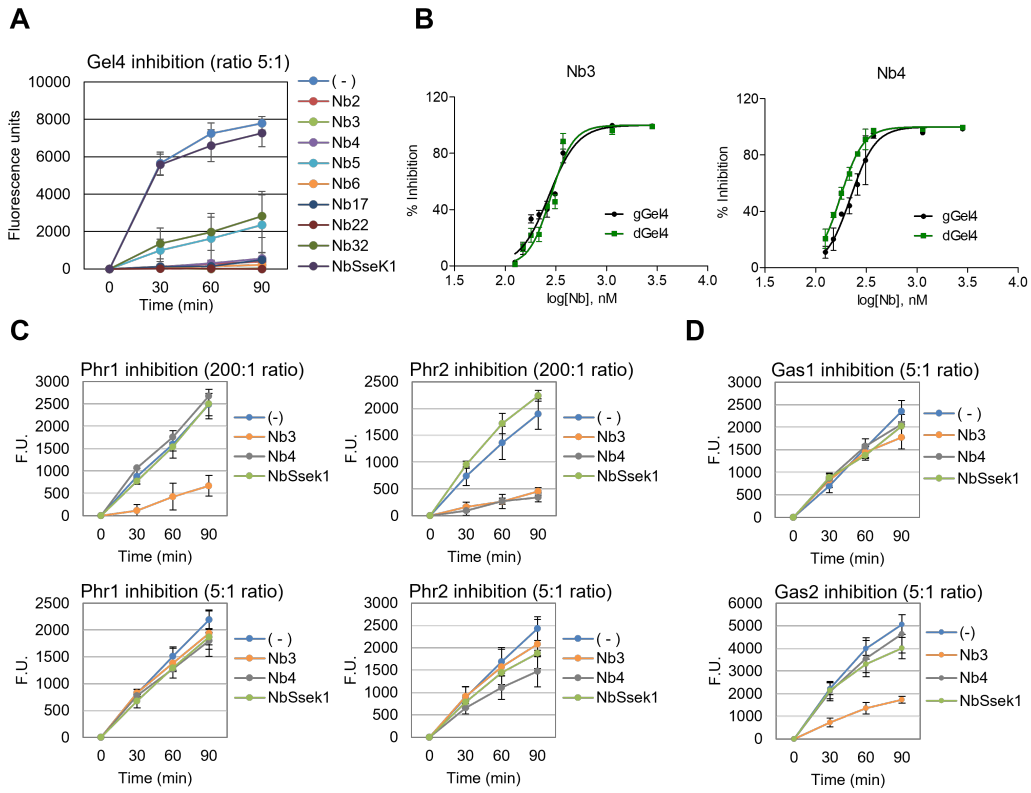

Figure S5. Gel4 and Gel orthologs inhibition by Nb3 and Nb4. (**A**) Inhibition time-course of gGel4 enzymatic activity by the complete set of Nbs. β-(1,3)-glucanosyl transglycosylase enzymatic activity was measured in the absence (-) or presence of 5-fold molar excess of the Nb. NbSseK1 which recognizes the non-related *Salmonella enterica* SseK1 protein was used as a negative control[31]. (**B**) The IC_{50} (nM) values for Nb3 and Nb4 against gGel4 and dGel4 were determined by using variable concentrations of the Nb3 and Nb4 (Nb3 and Nb4 concentrations ranged from 125 to 2850 nM while gGel4/dGel4 concentration was fixed at 420 nM) and under the same conditions as described in Methods. The reactions took place at 37ºC for 30 min. The IC_{50}s against gGel4 and dGel4 were 270.5 and 283.8 for Nb3, and 221.5 and 175.5 nM for Nb4, respectively. The IC_{50} sigmoidal curves were fit using data from at least three independent experiments using GraphPad Prism software. (**C**) Inhibition time-course of Phr1 and Phr2

enzymatic activity by Nb3 and Nb4 at 5-fold and 200-fold molar excess. Phr1 activity was measured at pH 7.2. (**D**) Inhibition time-course of Gas1 and Gas2 enzymatic activity by Nb3 and Nb4 at 5-fold molar excess. Data are shown as mean ± standard deviation (SD) from at least three independent experiments. F.U: Fluorescence arbitrary units.

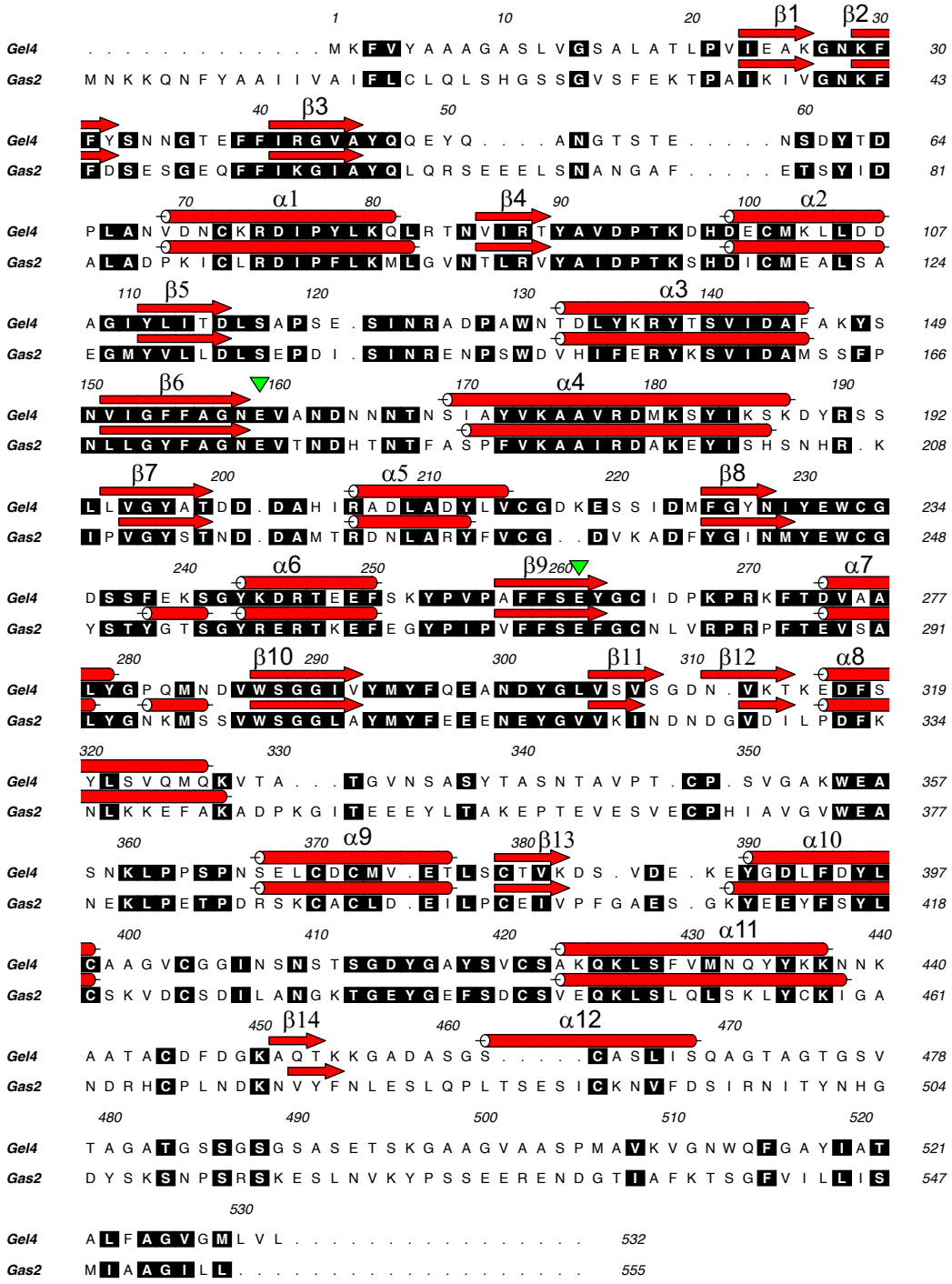

Figure S6. Sequence alignment of Gel4 and Gas2. Residues highlighted in black indicate that they are identical or highly similar. Note that for Gel4, only the residues present in the crystal structure are shown in the alignment while for Gas2, the entire sequence is shown. Shown above the sequences, in red, are the secondary structure elements (α-helices and β-strands) based on the Gel4 and Gas2 structures. The numbering for the secondary structure elements is only displayed for Gel4. The Glu residues involved

in catalysis, either acting as the acid/base (E159) or the nucleophilic residue (E261), are indicated with green inverted triangles. The catalytic and CBM43 domains for Gel4 are formed by residues 19-365 and 366-469, respectively.

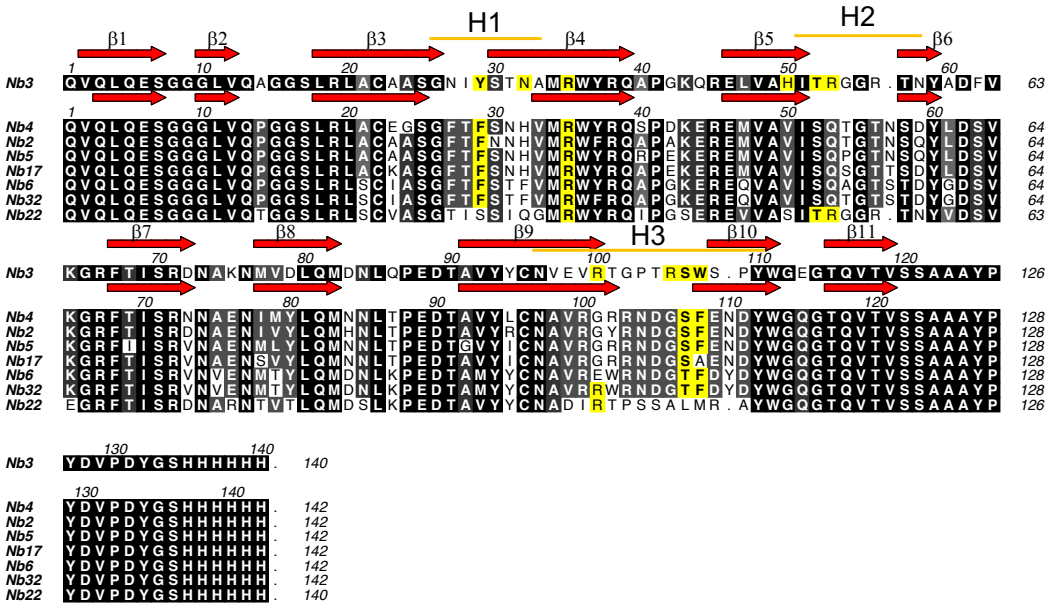

Figure S7. Multiple alignment of the selected anti-Gel4 Nbs displaying the Nb3 residues engaged in dGel4 recognition. The Nb3 residues that interact with dGel4 and the conservation with other Nbs are highlighted in yellow. The secondary structure elements (α-helices and β-strands) for Nb3 and Nb4 are shown in red. Note that the three hypervariable loops not only encompass loops but also a few residues of the adjacent secondary structures.

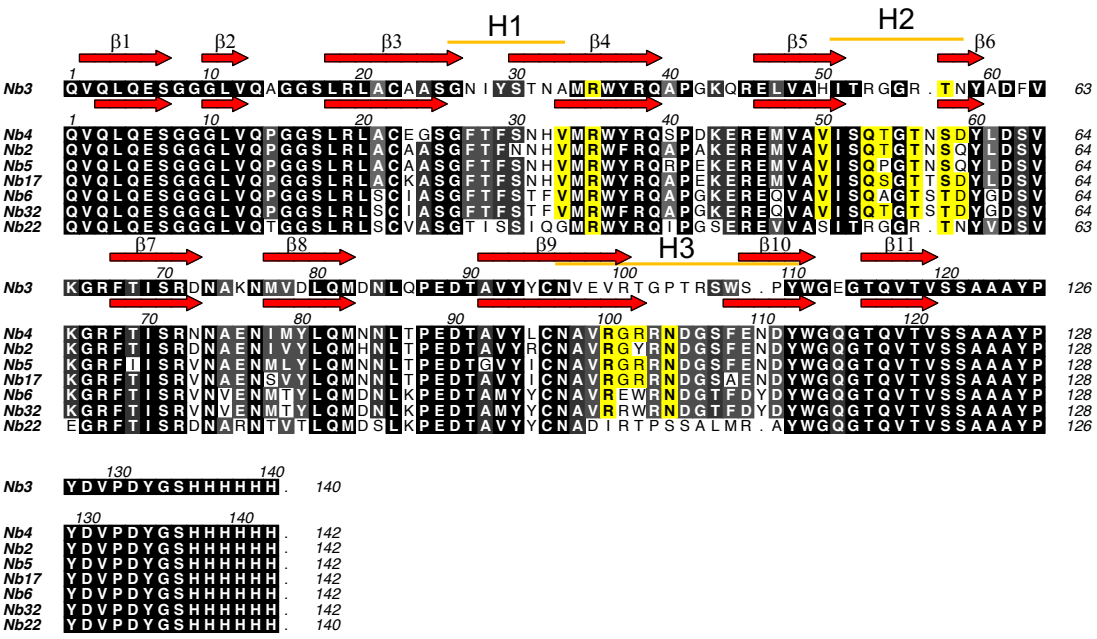

Figure S8. Multiple alignment of the selected anti-Gel4 Nbs displaying the Nb4 residues engaged in dGel4 recognition. The Nb4 residues that interact with dGel4 and the conservation with other Nbs are highlighted in yellow. The secondary structure elements (α-helices and β-strands) for Nb3 and Nb4 are shown in red.

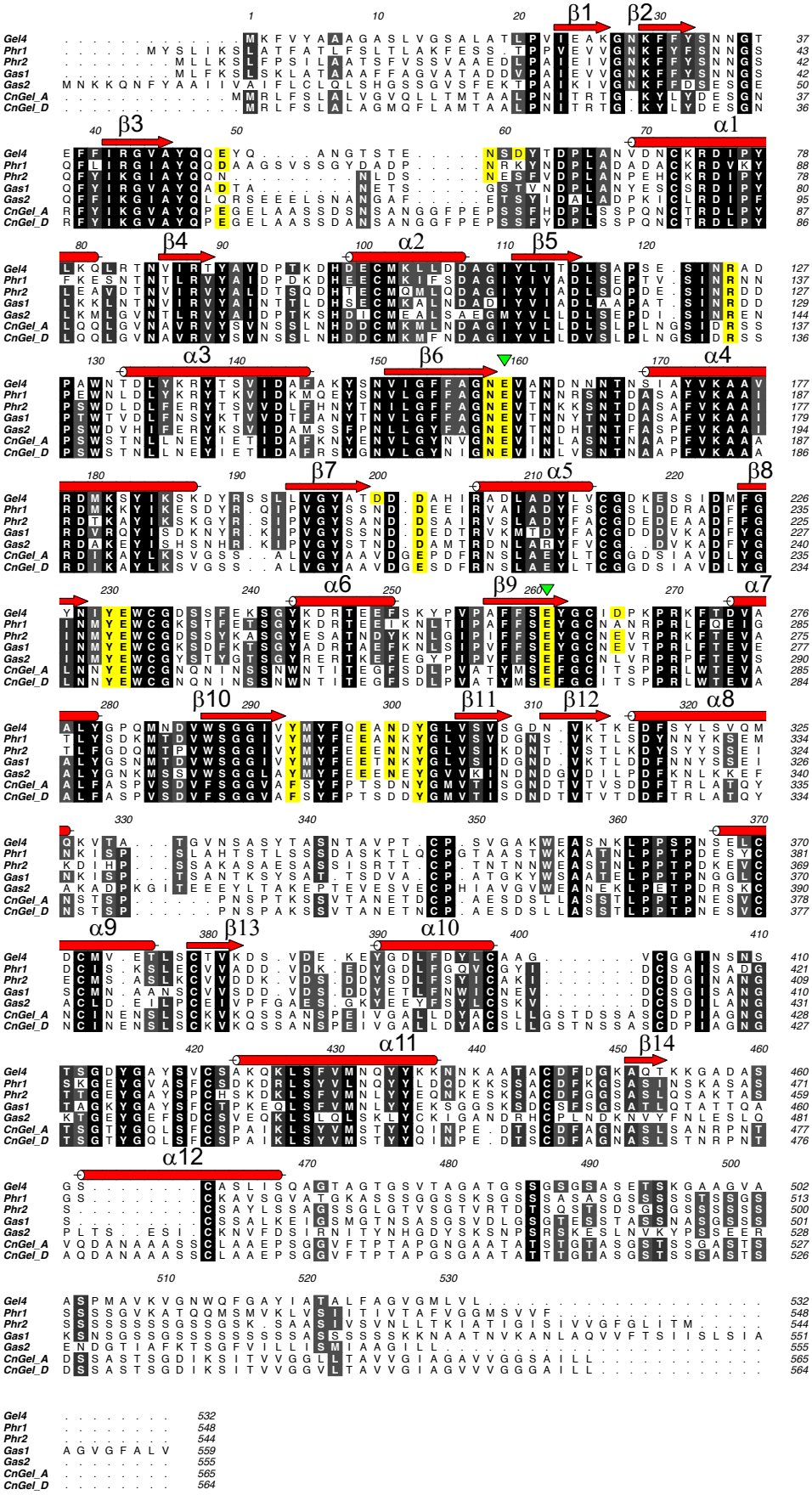

Figure S9. Multiple sequence alignment of Gel4, Phr1, Phr2, Gas1, Gas2 and *Cn*Gel

from *C. neoformans* (*Cn*Gel_A) and *C. deneoformans* (*Cn*Gel_D). Secondary structure elements from the dGel4 structure are shown, with α-helices and β-strands in red. The dGel4 residues that interact with Nb3 and the conservation with other Gel4 orthologs based on these interactions are highlighted in yellow. The Glu residues that are involved in catalysis, either acting as the acid/base (E159) or the nucleophilic residue (E261), are indicated with green inverted triangles. Note that *Cn*Gel stands for *Cryptococcus spp* Gel, a very similar enzyme to Gel4 that is present in this fungus. A blast search using the Gel4 catalytic domain against the *C. neoformans* genome revealed that *Cn*Gel appears to be the only member of this type of enzymes in this organism. The sequences of *Cn*Gel from H99 (*C. neoformans*, *Cn*Gel_A) and JEC21 (*C. deneoformans*, CnGel_D) are shown. Residues are color-coded by the degree of sequence conservation where black and grey colors denote identity/high similarity and similarity, respectively.

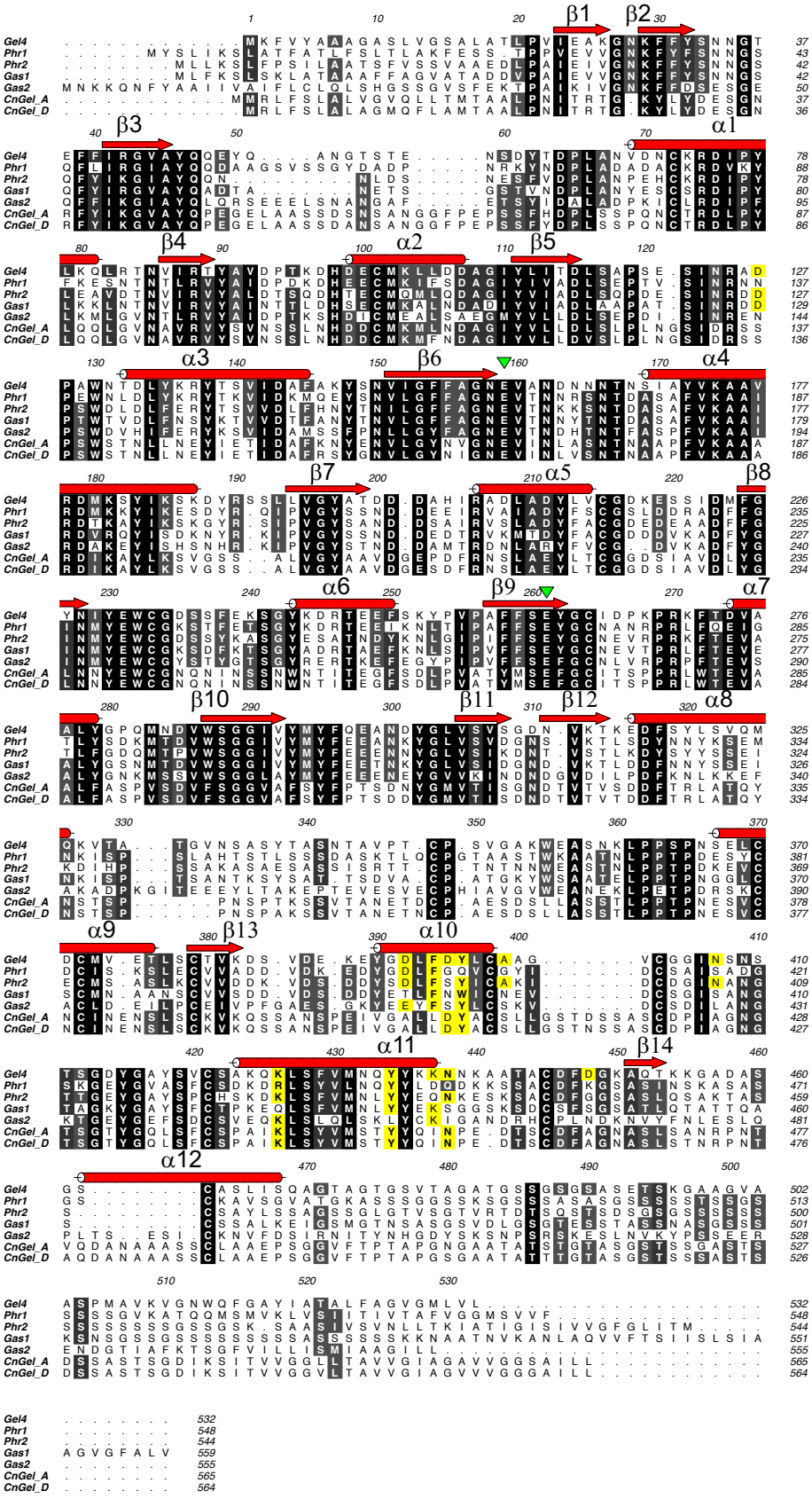

Figure S10. Multiple sequence alignment of Gel4, Phr1, Phr2, Gas1, Gas2 and *Cn*Gel from *C. neoformans* (*Cn*Gel_A) and *C. deneoformans* (*Cn*Gel_D). Secondary structure

elements from the dGel4 structure are shown, with α-helices and β-strands in red. The dGel4 residues that interact with Nb4 and the conservation with other Gel4 orthologs based on these interactions are highlighted in yellow. The Glu residues that are involved in catalysis, either acting as the acid/base (E159) or the nucleophilic residue (E261), are indicated with green inverted triangles. Residues are color-coded by the degree of sequence conservation where black and grey colors denote identity/high similarity and similarity, respectively.

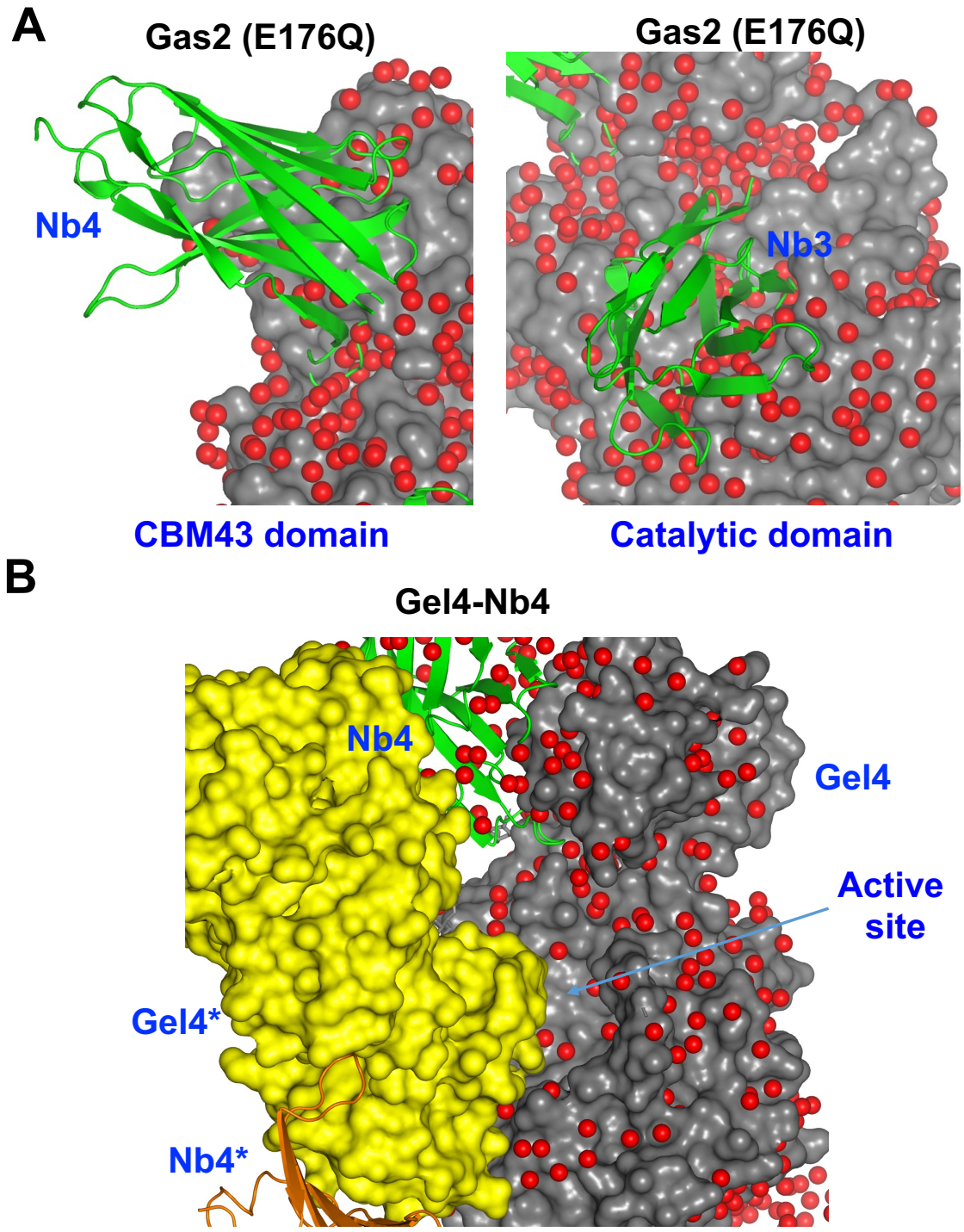

Figure S11. Analysis of the water molecules around the active site of β-1,3-glucanosyltransferases. (A) Crystal structure of the Gas2 E176Q mutant showing the surface water molecules in the CBM43 and the catalytic domain. Additionally, Nb3 and Nb4 from the crystal structures of dGel4-Nb3 and dGel4-Nb4 complexes were

superimposed onto the Gas2 E176Q mutant structure (PDB entry 2W61) to pinpoint the Nbs with respect to the surface water molecules. The water molecules are shown as red spheres. This structure evidences the large number of water molecules that will be likely released upon binding of Nb3 to the Gel4 active site. On the contrary, Nb4 will release a limited number of water molecules, which might explain why Nb4 is majorly enthalpically driven. (**B**) The structure of dGel4-Nb4 reveals that a neighbouring dGel4* (yellow) from another asymmetric unit occupies the dGel4 active site (grey), thus blocking the access of water molecules to most of the active site and hindering the examination of the active site's water molecules.

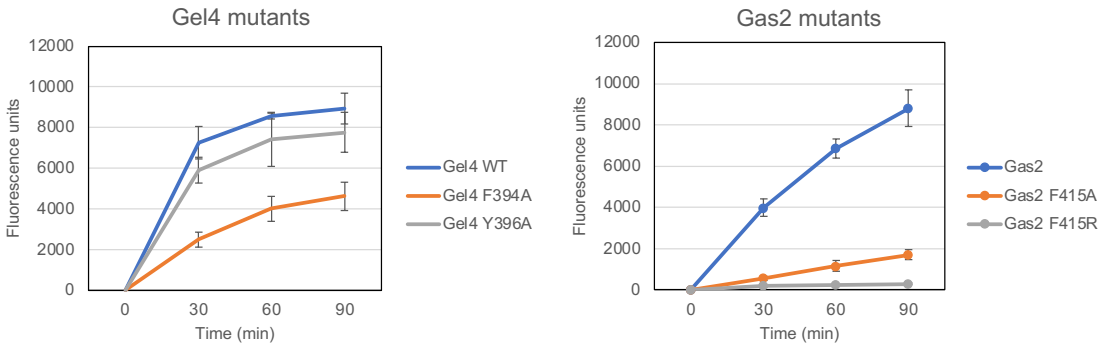

Figure S12. Time-course of gGel4, Gas2, and mutants enzymatic activity. Note that the activity for Gel4 and mutants was determined in triplicate, while the activity with Gas2 and mutants was determined in duplicate. An example of one of these experiments is shown for Gas2 and F415A/R mutants. Data are shown as mean ± standard deviation (SD).

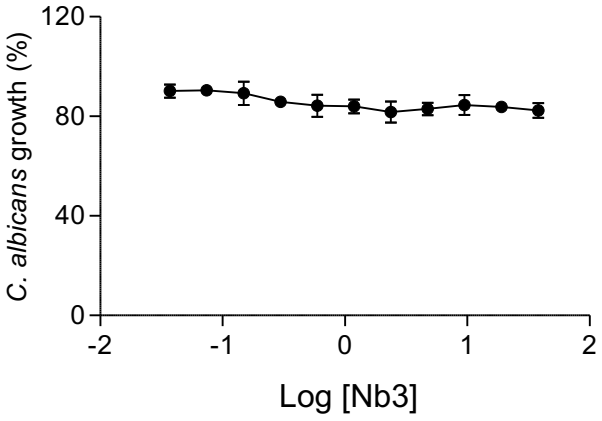

Figure S13. Nb3 sensitivity of *C. albicans*. The antifungal activity of a variable range of Nb3 against *C. albicans* strain CAF2-1, was measured in a 46 microtiter plate assay (see Methods) and presented as percentage growth compared to untreated controls. The experiments were performed at 37ºC. Data represent the mean and standard deviation of at least three independent experiments. The logarithmic values were obtained using the Nb3 concentration in μM.

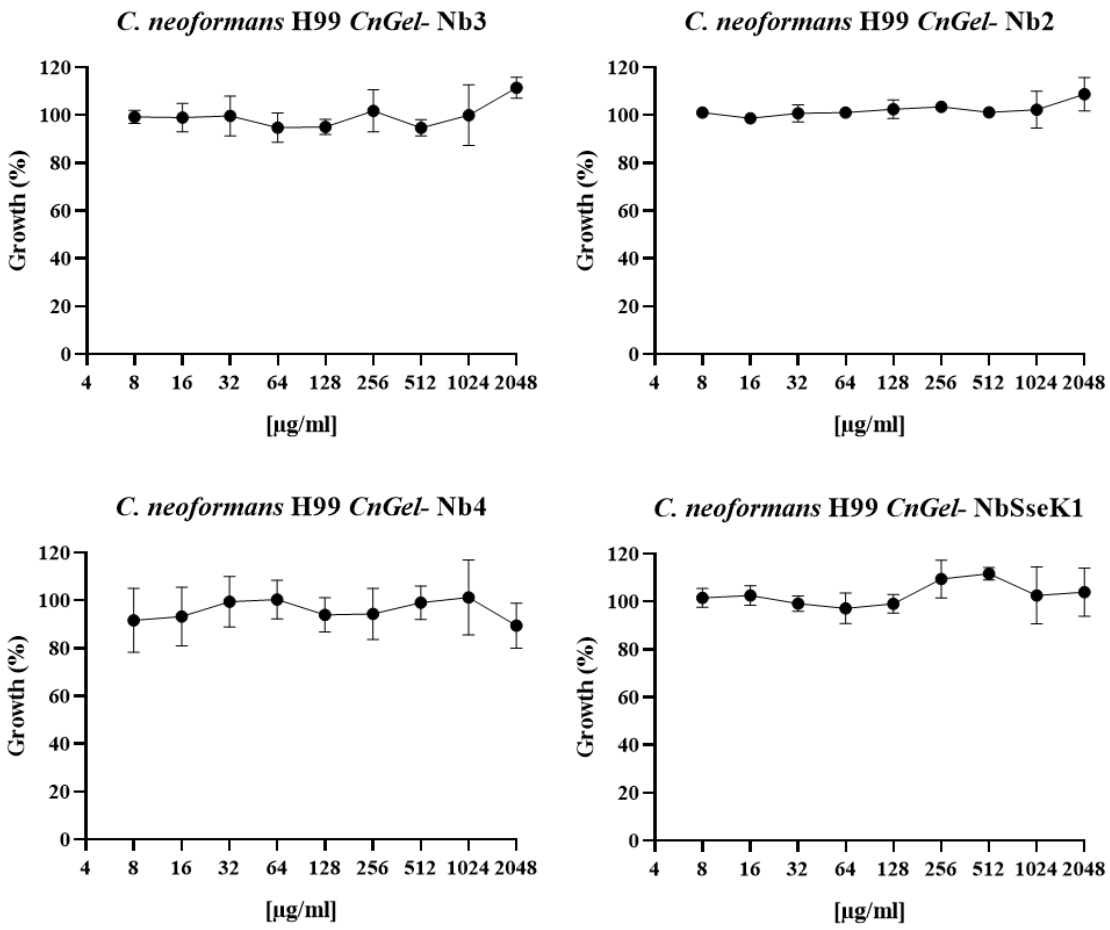

Figure S14. *In vitro* activity of Nb3, Nb2, Nb4, and NbSseK1 against the growth of *C. neoformans* H99 *CnGel-*. Colorimetric assays based on XTT reduction were performed as described in the Materials and Methods section. In these assays, *C. neoformans* H99 *CnGel*- was exposed to Nb2, Nb3, Nb4, and NbSseK1 at concentrations ranging from 4 µg/mL to 2048 µg/mL. The assays were carried out in 96-well microtiter plates at 30°C for 48 hours.

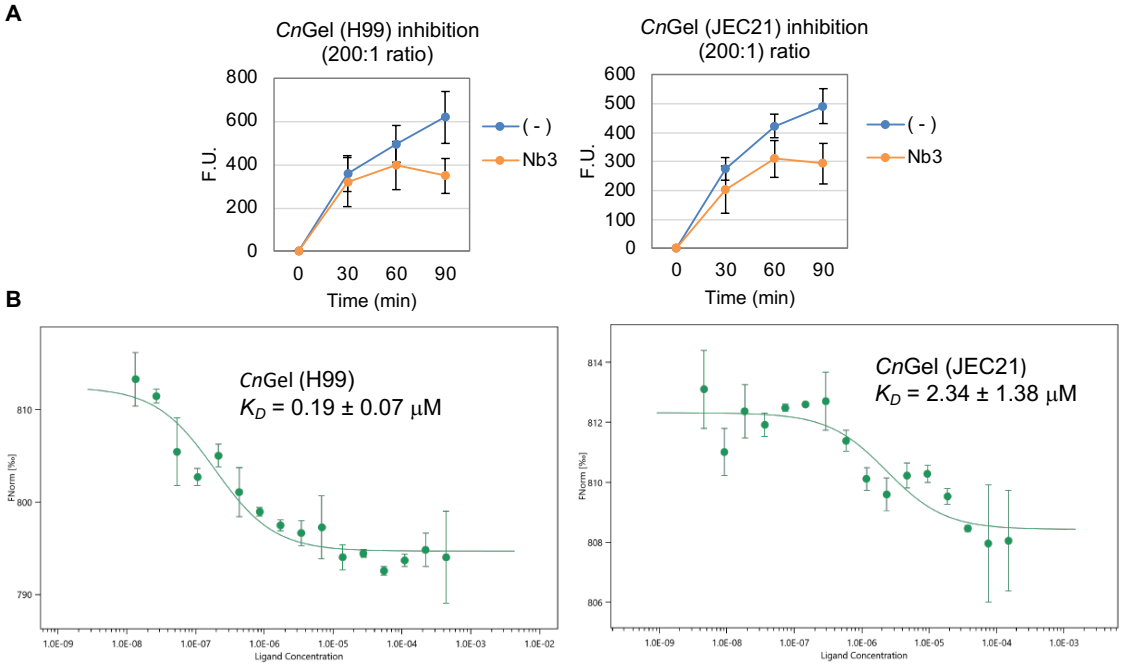

Figure S15. (**A**) Time-course of the enzymatic activity of *Cn*Gel from both strains. The activity was determined using 0.9 µM L6-SR as acceptor and 2.5 mg/mL laminarin as a donor in 50 mM citrate-phosphate buffer pH 7.2, in the absence (-) or presence of 200-fold molar excess of the Nb3. Data are shown as mean ± standard deviation (SD) from at least three independent experiments. **(B)** MST binding curve used to determine K_D for Nb3 against *Cn*Gel from both strains. Error represents SD between two separate experiments; K_D values ± SD are shown.

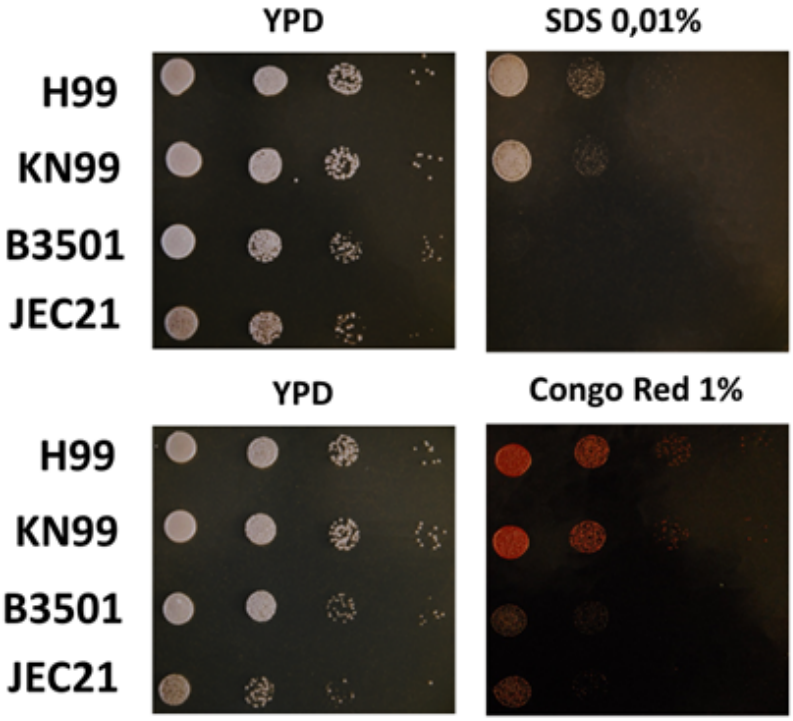

Figure S16. Sensitivity of *Cryptococcus deneoformans* B3501 and JEC21 strains and *Cryptococcus neoformans* H99 and KN99 strains to SDS and Congo Red. Cells were exponentially grown in YPD, and 1/10 dilution series of each strain were spotted onto YPD plates containing the indicated amounts of Congo Red and SDS.

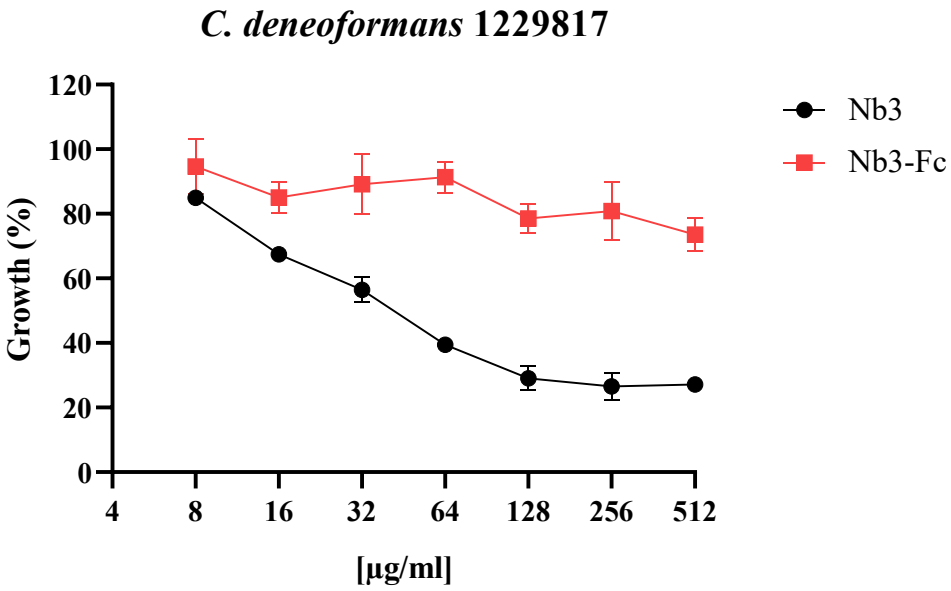

Figure S17. Sensitivity of *C. deneoformans* 1229817 to Nb3-Fc. Colorimetric assays based on XTT reduction were performed as described in the Materials and Methods section. *C. deneoformans* 1229817 was subjected to varying concentrations of Nb3-Fc, ranging from 4 µg/mL to 512 µg/mL. The assays were conducted in 96-well microtiter plates at a temperature of 30°C for 48 hours. The sensitivity for Nb3 is also shown for comparison purposes.

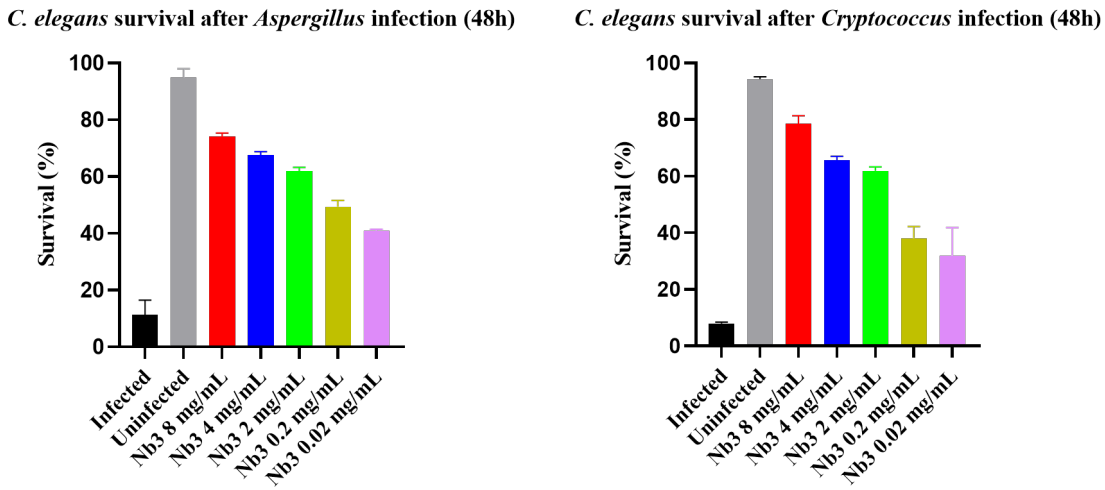

Figure S18. Efficacy of Nb3 in *C. elegans* of *A. fumigatus* and *C. neoformans* infection. The left panel shows the survival of *C. elegans* glp-4/sek-1 double mutants after infection with *A. fumigatus* B5233. Two thick drops of a highly concentrated conidial suspension were placed on an NGM agar plate with *C. elegans* L4 larvae and cultured overnight. The worms crawled over the conidial drops and ingested *A. fumigatus* spores. After infection, the worms were washed four times with M9 buffer to remove spores attached to their cuticles and cultured in 96-well plates containing 20% BHI broth with increasing concentrations of Nb3 in M9 buffer. Approximately 60 worms (3 wells) were assessed for each concentration. One-way ANNOVA P values for all groups vs. infected animals were < 0.0001. The right panel shows the survival of *C. elegans* glp-4/sek-1 double mutants after infection with *C. deneoformans* 1229817. A grass of *C. deneoformans* was added to an NGM plate to allow the worms to ingest fungal cells and cultured overnight. Four times washed L4 larvae were cultured with several Nb3 concentrations in 20% BHI broth diluted in M9 buffer. One-way ANNOVA p values for Nb3 8 mg/mL, 4 mg/mL and 2 mg/mL vs. infected animals were < 0.0001, while one-way ANNOVA p values for Nb3 0.2 mg/mL and 0.02 mg/mL were 0.0008 and 0.0033, respectively.

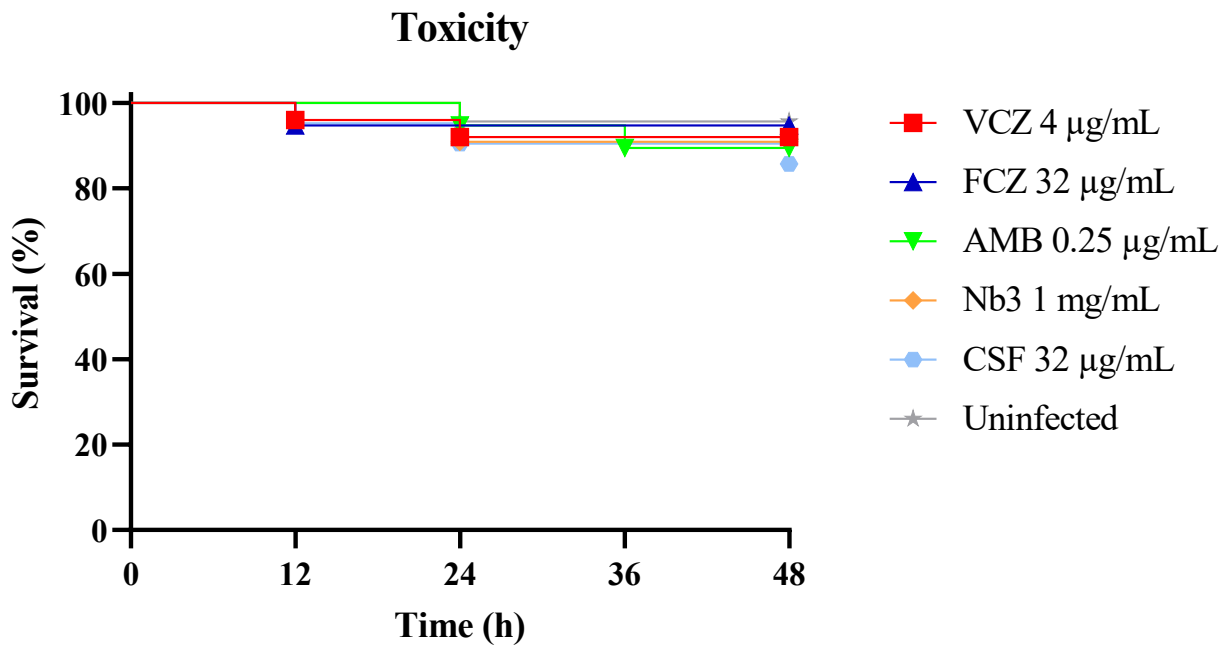

Figure S19. Toxicity of Nb3 and antifungal drugs in uninfected L4 worms. A total of ~100 worms were assessed for each concentration. Experiments were performed for 2 days at 25ºC and survival assessed every 12 h as described in Materials and Methods. Gehan-Breslow-Wilcoxon test was performed for all experiments ($p > 0.89$ for all drugs vs. uninfected worms).

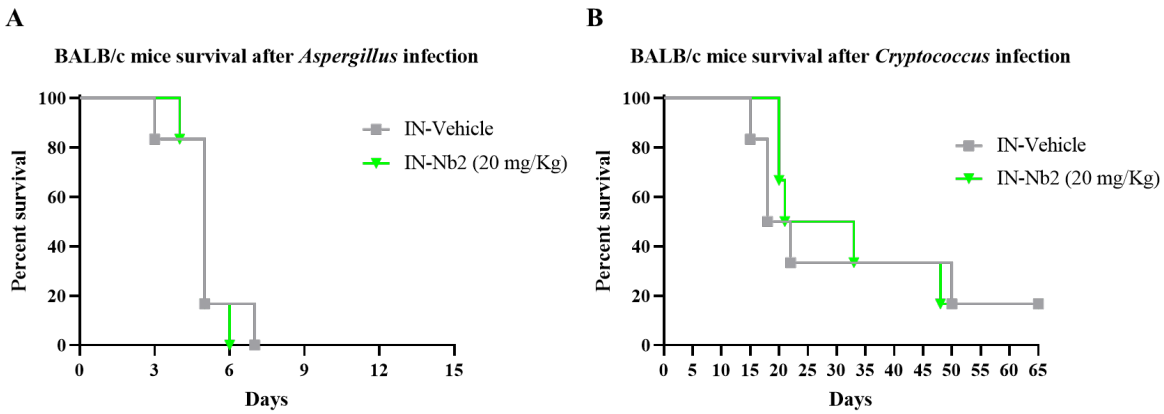

Figure S20. Survival of BALB/c mice infected with *A. fumigatus* B5233 (**A**) and *C. deneoformans* 1299817 (**B**), previously immunosuppressed with cyclophosphamide and/or hydrocortisone, and treated with Nb2 or vehicle which were IN administered. Results were analyzed using the Mantel-Cox test: p>0,67 in all cases.

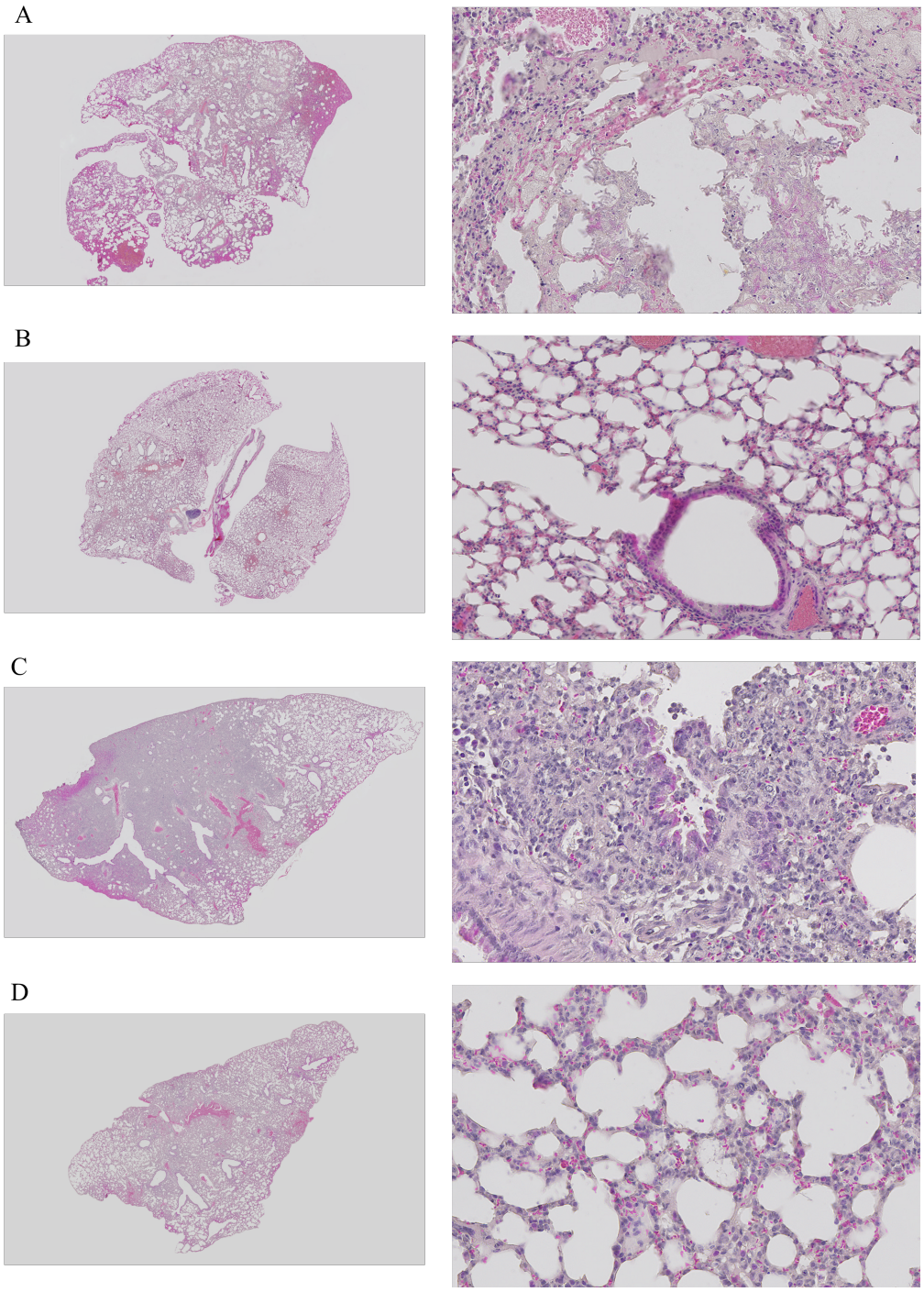

Figure S21. Hematoxylin-eosin stained histological slides were prepared from the lungs of mice infected with *A. fumigatus* B5233 (**A** and **B**) and *C. deneoformans* 1229817 (**C** and **D**). The mice were treated with either PBS (shown in panels **A** and **C**) or Nb3 (shown in panels **B** and **D**). The figures on the left correspond to a complete image of the histological section, while on the right, a more detailed image of the lung structure can be visualized.

Table S1. Thermodynamic parameters for Nbs binding to Gel4. K_D is the dissociation constant (=1/K), and ΔG, ΔH and -TΔS are the thermodynamic parameters. The stoichiometry of binding in all cases was close to ~1:1. The experiments were performed at 25°C in 25 mM Tris, 150 mM NaCl pH = 7.5. Note that the K_D of Nb22 is the best one towards the deglycosylated Gel4 while the K_D of Nb2 is the best one towards the glycosylated Gel4. Error values represent the error calculated through iteration fit of the data sets by the Origin 7 (Microcal).

Nb	Gel4 (forms)	K_D (nM)	ΔG (kcal/mol)	ΔH (kcal/mol)	-TΔS (kcal/mol)	n
2	Glycosylated	1.56 ± 0.22	-12.01	-26.32 ± 0.39	14.31	0.69
2	Deglycosylated	1.69 ± 0.53	-11.96	-24.24 ± 0.3	12.28	0.86
3	Glycosylated	8.69 ± 1.5	-10.94	6.66 ± 0.08	-17.60	0.74
3	Deglycosylated	3.24 ± 0.78	-11.53	9.37 ± 0.11	-20.90	1.07
4	Glycosylated	26.31 ± 5.95	-10.29	-33.74 ± 0.87	23.45	0.86
4	Deglycosylated	0.75 ± 0.2	-12.39	-28.3 ± 0.25	15.91	0.78
5	Glycosylated	73.82 ± 16.9	-9.68	-36.02 ± 1.6	26.34	0.98
5	Deglycosylated	19.74±5.18	-10.46	-7.93±0.9	-2-53	0.70
6	Glycosylated	575.02±173.7	-8.47	-0.76±0.11	-7.71	1.10
6	Deglycosylated	17.7±6.82	-11.81	-53.9±0.86	42.09	0.79
17	Glycosylated	17.7±4.92	-10.53	-20.32±0.6	9.79	0.90
17	Deglycosylated	3.79 ± 0.63	-11.65	-20.76 ± 0.84	9.11	0.78
22	Glycosylated	25.39 ± 7.67	-10.36	-10.64 ± 0.37	0.29	0.79
22	Deglycosylated	0.24 ± 0.05	-13.05	-10.9 ± 0.04	-2.15	0.71
32	Glycosylated	110.01 ± 22.14	-9.45	-22.64 ± 0.78	13.19	0.69
32	Deglycosylated	4.14 ± 1.21	-11.38	-15.88 ± 0.25	4.5	0.75

Table S2. Data collection and refinement statistics.

	Gel4 in complex with Nb3	Gel4 in complex with Nb4
Data collection		
Spacegroup	$P3_121$	$P2_12_12_1$
Cell dimensions		
a, *b*, *c* (Å)	96.99, 96.99, 106.62	85.39, 86.33, 178.33
α, β, γ (°)	90, 90, 120	90, 90, 90
Resolution (Å)	20-2.05 (2.16-2.05)*	20.00-1.90 (2.00-1.90)
R_{merge}	0.151 (0.991)	0.182 (1.588)
$I / \sigma I$	8.4 (1.8)	6.0 (1.0)
Completeness (%)	99.9 (100)	99.6 (99.7)
Redundancy	8.1 (6.8)	5.5 (5.5)
Mn(I) half-set correlation CC(1/2)	0.996 (0.603)	0.994(0.537)
Refinement		
Resolution (Å)	2.05	1.90
No. Unique reflections	36838	104001
R_{work} / R_{free}	0.172/0.206	0.215/0.264
No. atomsasymmetricunit		
Gel4	3505	7594
Nanobody 3	932	-
Nanobody 4	-	1933
GlcNAc	58	84
Mannose	43	88
Waters	180	689
Phosphate	10	-
B-factors (Å^2)		
Gel4	35.13	30.45
Nanobody 3	39.53	-
Nanobody 4	-	37.50
GlcNAc	58.26	47.95
Mannose	58.20	48.50
Waters	38.75	37.61
Phosphate	73.65	-
R.m.s. deviations		
Bond lengths (Å)	0.0103	0.0089
Bond angles (°)	1.78	1.60

1 crystal was used to determine each structure. *Values in parentheses are for the highest-resolution shell.

Table S3. Table of interactions between Gel4-Nb3/Nb4 interfaces residues.

Amino acid (Gel4)	Amino acid (Nb3)	Type of interaction
N158, E159 (backbone) R125 (side chain)	Y29 (sidechain) Y29 (backbone)	Hydrogen bond Hydrogen bond
Y302 (sidechain)	N32 (sidechain)	Hydrogen bond
D266 (sidechain)	R35 (sidechain)	Salt bridge
D266 (sidechain)	H50 (sidechain)	Hydrogen bond
E231 (sidechain)	T52 (backbone)	Hydrogen bond
E159, D200, D202 (side chain)	R53 (sidechain)	Salt bridge
E261 (sidechain)	R100 (sidechain)	Salt bridge
D61 (backbone) E49 (side chain) N59 (side chain and backbone)	R105 (side chain) R105 (side chain) R105 (sidechain)	Hydrogen bond Salt bridge Hydrogen bond
E49 (sidechain)	S106 (sidechain)	Hydrogen bond
E298 (sidechain)	S106 (sidechain)	Hydrogen bond
N300 (sidechain)	W107 (backbone)	Hydrogen bond
Y230 (sidechain)	W107 (sidechain)	Hydrogen bond
Y293, Y302 (sidechain)	W107 (sidechain)	CH-π

Amino acid (Gel4)	Amino acid (Nb4)	Type of interaction
A399, Y396 (sidechain)	V33 (sidechain)	CH-CH
A399 (backbone)	R35 (sidechain)	Hydrogen bond
A399 (side chain) Y396 (side chain)	V50 (sidechain)	CH-CH CH-π
D392 (backbone)	Q53 (sidechain)	Hydrogen bond
D448 (sidechain)	T54 (sidechain)	Hydrogen bond
D448 (sidechain)	T56 (sidechain)	Hydrogen bond
Y396, Y434 (sidechain)	S58 (backbone)	Hydrogen bond
D392, Y396 (side chain) K437 (side chain) N438 (sidechain)	D59 (backbone) D59 (side chain) D59 (sidechain)	Hydrogen bond Salt bridge Hydrogen bond
D392 (sidechain)	R100 (sidechain)	Salt bridge
D395 (sidechain)	G101 (backbone)	Hydrogen bond
D395 (side chain) N407 (side chain) F394 (sidechain)	R102 (backbone) R102 (side chain) R102 (sidechain)	Hydrogen bond Salt bridge Cation-π
D127, K426 (sidechain)	N104 (sidechain)	Hydrogen bond

Table S4. MIC_{50} values for the dose-response curves. The MIC_{50} is the minimum concentration of inhibitor required to reduce growth by at least 50%. This table shows MIC_{50} Nb3 ranges for several *A. fumigatus*, *C. albicans,* and *C. neoformans* species complex strains and/or isolates from at least three-four independent experiments.

Organism	**Nb3 MIC_{50} [µg/ml]**
A. fumigatus B5233	512
A. fumigatus 1631562	64 to 256
A. fumigatus 1677095	512 to1024
A. fumigatus 1627666	128 to512
A. fumigatus 838	512
A. fumigatus 286	1024 to 2048
A. fumigatus 678715 (VRZ resistant)	512
C. deneoformans 1229817	64
C. deneoformans B3501	1024
C. deneoformans JEC21	32 to64
C. deneoformans 24067	1024
C. neoformans KN99	>2048
C. neoformans H99	>2048
C. neoformans H99 *Cn*Gel-	>2048

Table S5. Antifungal susceptibility profile of main organisms of this work. This table shows MIC_{50} values of common drugs used in treatment of fungal infections for the main organisms of this work.

		MIC_{50} [µg/ml]			
Organism	**Nb3**	**CSF**	**VCZ**	**FCZ**	**AMB**
A. fumigatus B5233	512	32	0.5	ND	1
C. deneoformans 1229817	64	64	ND	> 64	0.25
C. neoformans H99	>2048	512	ND	> 64	0.25

Table S6. Sinergy of Nb3 in combination with voriconazole, fluconazole and amphotericin B according to the FICI method in cultures of *A. fumigatus* B5233, *C. neoformans* H99 and *C. deneoformans* 1229817.

Organism	Drug combination (AF1 + AF2)	AF1 MIC_{50} [µg/ml]	AF2 MIC_{50} [µg/ml]	AF1 combMIC_{50} [µg/ml]	AF2 combMIC_{50} [µg/ml]	FICI	Interpretation
A. fumigatus B5233	Nb3 + AMB	512	1	128	0.125	0.375	Synergy
A. fumigatus B5233	Nb3 + VCZ	512	0.5	1	0.25	0.502	Additive
A. fumigatus B5234	Nb3 + Nb4	512	512	16	16	0.063	Synergy
C. deneoformans 1229817	Nb3 + AMB	64	0.25	32	0,125	1.000	Additive
C. deneoformans 1229817	Nb3 + FCZ	64	64	32	2	0.531	Additive
C. deneoformans 1229817	Nb3 + Nb4	64	512	32	64	0.625	Additive
C. neoformans H99	Nb3 + AMB	512	0,25	4	0.125	0.508	Additive
C. neoformans H99	Nb3 + FCZ	512	64	512	64	2.000	Indifferent
C. neoformans H99	Nb3 + Nb4	512	512	256	16	0.531	Additive

References

[1] aK. J. Kwon-Chung, J. C. Edman, B. L. Wickes, *Infect Immun* **1992**, *60*, 602-605; bJ. Heitman, B. Allen, J. A. Alspaugh, K. J. Kwon-Chung, *Fungal Genet Biol* **1999**, *28*, 1-5.

[2] K. J. Kwon-Chung, *Mycologia* **1976**, *68*, 821-833.

[3] D. E. Wilson, J. E. Bennett, J. W. Bailey, *Proc Soc Exp Biol Med* **1968**, *127*, 820-823.

[4] K. Nielsen, G. M. Cox, P. Wang, D. L. Toffaletti, J. R. Perfect, J. Heitman, *Infect Immun* **2003**, *71*, 4831-4841.

[5] J. R. Perfect, S. D. Lang, D. T. Durack, *Am J Pathol* **1980**, *101*, 177-194.

[6] Y. C. Chang, B. L. Wickes, K. J. Kwon-Chung, *Gene* **1995**, *167*, 179-183.

[7] W. A. Fonzi, M. Y. Irwin, *Genetics* **1993**, *134*, 717-728.

[8] W. Kabsch, *Acta Crystallogr D Biol Crystallogr* **2010**, *66*, 125-132.

[9] A. Waterhouse, M. Bertoni, S. Bienert, G. Studer, G. Tauriello, R. Gumienny, F. T. Heer, T. A. P. de Beer, C. Rempfer, L. Bordoli, R. Lepore, T. Schwede, *Nucleic Acids Res* **2018**, *46*, W296-W303.

[10] M. D. Winn, C. C. Ballard, K. D. Cowtan, E. J. Dodson, P. Emsley, P. R. Evans, R. M. Keegan, E. B. Krissinel, A. G. Leslie, A. McCoy, S. J. McNicholas, G. N. Murshudov, N. S. Pannu, E. A. Potterton, H. R. Powell, R. J. Read, A. Vagin, K. S. Wilson, *Acta Crystallogr D Biol Crystallogr* **2011**, *67*, 235-242.

[11] A. J. McCoy, *Acta Crystallogr D Biol Crystallogr* **2007**, *63*, 32-41.

[12] P. Emsley, K. Cowtan, *Acta Crystallogr D Biol Crystallogr* **2004**, *60*, 2126-2132.

[13] G. N. Murshudov, P. Skubak, A. A. Lebedev, N. S. Pannu, R. A. Steiner, R. A. Nicholls, M. D. Winn, F. Long, A. A. Vagin, *Acta Crystallogr D Biol Crystallogr* **2011**, *67*, 355-367.

[14] C. Vincke, C. Gutierrez, U. Wernery, N. Devoogdt, G. Hassanzadeh-Ghassabeh, S. Muyldermans, *Methods Mol Biol* **2012**, *907*, 145-176.

[15] E. Romao, V. Poignavent, C. Vincke, C. Ritzenthaler, S. Muyldermans, B. Monsion, *Methods Mol Biol* **2018**, *1701*, 169-187.

[16] aI. Delso, J. Valero-Gonzalez, F. Gomollon-Bel, J. Castro-Lopez, W. Fang, I. Navratilova, D. M. F. van Aalten, T. Tejero, P. Merino, R. Hurtado-Guerrero, *ChemMedChem* **2018**, *13*, 128-132; bK. Kovacova, G. Degani, E. Stratilova, V. Farkas, L. Popolo, *FEMS Yeast Res* **2015**, *15*.

[17] aM. Mazan, N. Blanco, K. Kovacova, Z. Firakova, P. Rehulka, V. Farkas, J. Arroyo, *Biochem J* **2013**, *455*, 307-318; bM. Mazan, E. Ragni, L. Popolo, V. Farkas, *Biochem J* **2011**, *438*, 275-282.

[18] N. Collaborative Computational Project, *Acta Crystallogr D Biol Crystallogr* **1994**, *50*, 760-763.

[19] J. A. Sugui, J. Pardo, Y. C. Chang, A. Mullbacher, K. A. Zarember, E. M. Galvez, L. Brinster, P. Zerfas, J. I. Gallin, M. M. Simon, K. J. Kwon-Chung, *Eukaryot Cell* **2007**, *6*, 1552-1561.

[20] F. J. Walton, A. Idnurm, J. Heitman, *Mol Microbiol* **2005**, *57*, 1381-1396.

[21] F. Moyrand, T. Fontaine, G. Janbon, *Mol Microbiol* **2007**, *64*, 771-781.

[22] J. Meletiadis, S. Pournaras, E. Roilides, T. J. Walsh, *Antimicrob Agents Chemother* **2010**, *54*, 602-609.

[23] A. Casadevall, J. Mukherjee, S. J. Devi, R. Schneerson, J. B. Robbins, M. D. Scharff, *J Infect Dis* **1992**, *165*, 1086-1093.

[24] I. Okoli, E. M. Bignell, *British Microbiology Research Journal* **2015**, *7*, 93-99.
[25] M. J. Beanan, S. Strome, *Development* **1992**, *116*, 755-766.
[26] D. H. Kim, R. Feinbaum, G. Alloing, F. E. Emerson, D. A. Garsin, H. Inoue, M. Tanaka-Hino, N. Hisamoto, K. Matsumoto, M. W. Tan, F. M. Ausubel, *Science* **2002**, *297*, 623-626.
[27] M. Porta-de-la-Riva, L. Fontrodona, A. Villanueva, J. Ceron, *J Vis Exp* **2012**, e4019.
[28] B. Xu, Q. Luo, Y. Gong, J. Li, J. Cao, *Infect Immun* **2021**, *89*.
[29] S. Muyldermans, *Annu Rev Biochem* **2013**, *82*, 775-797.
[30] A. M. Gonzalez-Ramirez, A. S. Grosso, Z. Yang, I. Companon, H. Coelho, Y. Narimatsu, H. Clausen, F. Marcelo, F. Corzana, R. Hurtado-Guerrero, *Nat Commun* **2022**, *13*, 2398.
[31] J. B. Park, Y. H. Kim, Y. Yoo, J. Kim, S. H. Jun, J. W. Cho, S. El Qaidi, S. Walpole, S. Monaco, A. A. Garcia-Garcia, M. Wu, M. P. Hays, R. Hurtado-Guerrero, J. Angulo, P. R. Hardwidge, J. S. Shin, H. S. Cho, *Nat Commun* **2018**, *9*, 4283.